Technology Collaboration Programme
by IEA

International Energy Agency
Photovoltaic Power Systems Programme

Task 13 Reliability and Performance of Photovoltaic Systems

PVPS

Operational and Economic Impacts of Extreme Weather on PV Power Plants

2025

Report IEA-PVPS T13-33:2025

What is IEA PVPS TCP?

The International Energy Agency (IEA), founded in 1974, is an autonomous body within the framework of the Organisation for Economic Cooperation and Development (OECD). The Technology Collaboration Programmes (TCP) were created with a belief that the future of energy security and sustainability starts with global collaboration. The programmes are made up of 6.000 experts across government, academia, and industry dedicated to advancing common research and the application of specific energy technologies.

The IEA Photovoltaic Power Systems Programme (IEA PVPS) is one of the TCPs within the IEA and was established in 1993. The mission of the programme is to "enhance the international collaborative efforts which facilitate the role of photovoltaic solar energy as a cornerstone in the transition to sustainable energy systems." To achieve this, the programme's participants have undertaken a variety of joint research projects in PV power systems applications. The overall programme is headed by an Executive Committee, comprised of one delegate from each country or organisation member, which designates distinct 'Tasks,' that may be research projects or activity areas.

The 28 IEA PVPS participating countries are Australia, Austria, Belgium, Canada, China, Denmark, Finland, France, Germany, India, Israel, Italy, Japan, Korea, Lithuania, Malaysia, Morocco, the Netherlands, Norway, Portugal, South Africa, Spain, Sweden, Switzerland, Thailand, Türkiye, the United Kingdom and the United States of America. The European Commission, Solar Power Europe and the Solar Energy Research Institute of Singapore are also members.

Visit us at: www.iea-pvps.org

What is IEA PVPS Task 13?

Within the framework of IEA PVPS, Task 13 aims to provide support to market actors working to improve the operation, the reliability and the quality of PV components and systems. Operational data from PV systems in different climate zones compiled within the project will help provide the basis for estimates of the current situation regarding PV reliability and performance.

The general setting of Task 13 provides a common platform to summarize and report on technical aspects affecting the quality, performance, reliability and lifetime of PV systems in a wide variety of environments and applications. By working together across national boundaries, we can all take advantage of research and experience from each member country and combine and integrate this knowledge into valuable summaries of best practices and methods for ensuring PV systems perform at their optimum and continue to provide competitive return on investment.

Task 13 has so far managed to create the right framework for the calculations of various parameters that can give an indication of the quality of PV components and systems. The framework is now there and can be used by the industry who has expressed appreciation towards the results included in the high-quality reports.

The IEA PVPS countries participating in Task 13 are Australia, Austria, Belgium, Canada, Chile, China, Denmark, Finland, France, Germany, Israel, Italy, Japan, the Netherlands, Norway, Spain, Sweden, Switzerland, Thailand, and the United States of America, and the Solar Energy Research Institute of Singapore.

SUGGESTED CITATION

Burnham, L., Tanahashi, T. (2025). Burnham, L., Tanahashi, T., Jahn, U. (Eds.), *Operational and Economic Impacts of Extreme Weather on PV Power Plants* (Report No. T13-33:2025). IEA PVPS Task 13. https://doi.org/10.69766/FFNG4976

COVER PICTURE

Damages to a PV plant from Hurricane Milton, which swept across the southeastern US in 2024, are attributable to a poorly engineered single-axis tracker system (Credit: Laurie Burnham, Sandia National Laboratories).

INTERNATIONAL ENERGY AGENCY

PHOTOVOLTAIC POWER SYSTEMS PROGRAMME

IEA PVPS Task 13

Reliability and Performance
of Photovoltaic Systems

Operational and Economic Impacts of Extreme Weather on PV Power Plants

Report IEA-PVPS T13-33:2025

December 2025

ISBN: 978-1-7642902-4-1

DOI: https://doi.org/10.69766/FFNG4976

AUTHORS

Main Authors

Laurie Burnham, Sandia National Laboratories, USA

Tadanori Tanahashi, National Institute of Advanced Industrial Science and Technology (AIST), Japan

John Sedgwick, VDE Americas, USA

Christopher Baldus-Jeursen, Natural Resources Canada - CanmetENERGY, Canada

Alexander Granlund, RISE Research Institutes of Sweden, Sweden

Leonardo Micheli, Sapienza University of Rome, Italy

Anna Heimsath, Fraunhofer Institute for Solar Energy Systems ISE, Germany

Narendra Shiradkar, Indian Institute of Technology Bombay, India

Contributing Authors

John Allen, Central Michigan University, USA

Evelyn Bamberger, OST Eastern Switzerland University of Applied Sciences, Switzerland

Peter Bostock, VDE Americas, USA

David Brearley, VDE Americas, USA

Christof Bucher, Berner Fachhochschule, Switzerland

Brahim Aissa, Qatar Environment & Energy Re-search Institute, Qatar

Ricardo Conceição, IMDEA Energy, Spain

Benjamin Figgis, Qatar Environment & Energy Re-search Institute, Qatar

Juan Lopez Garcia, Qatar Environment & Energy Re-search Institute, Qatar

Thore Müller, PVRADAR Labs GmbH, Germany

Dhanup S. Pillai, Qatar Environment & Energy Re-search Institute, Qatar

Mariella Rivera, Fraunhofer Institute for Solar Energy Systems ISE, Germany

Bram Hoex, University of New South Wales (UNSW), Australia

David Moser, European Academy Bozen/Bolzano (EURAC), Italy

Editors

Laurie Burnham, Sandia National Laboratories, USA

Tadanori Tanahashi, National Institute of Advanced Industrial Science and Technology (AIST), Japan

Ulrike Jahn, Fraunhofer Center for Silicon Photovoltaics CSP, Germany

TABLE OF CONTENTS

ACKNOWLEDGEMENTS

This paper's main authors want to acknowledge the many valuable and much appreciated contributions to this report made by IEA-PVPS Task 13 members and other international experts. In addition, the authors especially thank the following individuals for their thorough review of this report: Lenny Tinker (Solar Energy Technologies Office, U.S. Department of Energy, USA), Yves Poissant (Natural Resources Canada – CanmetENERGY, Canada), Minoru Kobayashi (NEDO, Japan), and Bert Herteleer (SUPSI, Switzerland) for their thoughtful and insightful reviews, which significantly enhanced the overall quality of the report. We also extend our gratitude to Franz Baumgartner and Markus Klenk (ZHAW, Switzerland) for reviewing a portion of the report.

This report and the work reflected therein is supported by numerous governmental agencies, including:

The German Federal Ministry for Economic Affairs and Climate Action (BMWK) under contract no. 03EE1120B.

The U.S. Department of Energy's Office of Energy Efficiency and Renewable Energy (EERE) under the Solar Energy Technologies Office Award Numbers 38268, 38535 and 52773.

The New Energy and Industrial Technology Development Organization (NEDO), Japan, under contract # 20000860-0.

The Sole4PV, a project funded by the Italian Ministry of University and Research under the "Rita Levi di Montalcini" 2019 grant.

The Swedish Energy Agency under work order 177609.

LIST OF ABBREVIATIONS

AOD	Aerosol optical depth
BOS	Balance of system
CAPEX	Capital expenditure
DHI	Direct horizontal irradiance
DOD	Dust optical depth
DSS	Dust and sandstorms
ECMWF	European Centre for Medium-Range Weather Forecasts
EL	Electroluminescence
GHI	Global horizontal irradiance
IP	Ingress protection
IPCC	Intergovernmental Panel on Climate Change
IR	Infrared
Isc	Short circuit current
LCOE	Levelized cost of energy
LiDAR	Light detection and ranging
MPPT	Maximum power point tracking
NOAA	U.S. National Oceanic and Atmospheric Administration
O&M	Operations and maintenance
OPEX	Operational expenditure
PID	Potential-induced degradation
POA	Plane-of-array
$PM_{2.5}$	Airborne particulate matter with a diameter 2.5 µm and smaller
PM_{10}	Airborne particulate matter with a diameter 10 µm and smaller
PV	Photovoltaic
PVpot	Potential PV production
Rd	Degradation rate
RCP	Rapid Concentration potential
ROCC	Remote operation control centre
RTC	Regional Test Center
SAT	Surface air temperature
SCADA	Supervisory Control and Data Acquisition
SCB	String combiner box
TAS	Temperature-at-surface
TC	Temperature coefficient
TW	Terawatt
Voc	Open-circuit voltage

EXECUTIVE SUMMARY

In an anthropocentric world increasingly defined by changes in atmospheric chemistry, two clear trends have emerged. One is the increase in the frequency and severity of extreme and anomalous weather events, the latter driven by rising temperatures and changing patterns of humidity and precipitation; the other is the rapid acceleration of photovoltaic (PV) capacity, including the spread of PV into new climate zones, with 2 terawatts (TW) deployed across six continents in 2024, and on course for an expected 8 TW by 2030.

To ensure the further growth of PV energy generation worldwide requires attention be paid to global climate trends and to opportunities for designing PV systems to withstand and quickly recover from specific storm threats. Traditionally, solar technologies have been a one-size-fits-all commodity, and specific climatic stressors have been a minor consideration in module and system design. As solar installations proliferate across almost all climate zones, however, design optimization for specific weather threats is gaining attention. This report provides a comprehensive look at changing weather patterns and their anticipated impact on the reliability and performance of PV systems worldwide. Broken down by storm category, the report covers extreme weather events of greatest significance to PV power plants: tropical cyclones, convective storms, snowstorms, dust storms, heat waves, floods and wildfires. For each category, an overview of the threat landscape is provided, along with best practices for design and procurement, mitigation strategies, post-storm assessment and follow-on operation and maintenance (O&M) strategies.

The report also considers weather-inflicted damages to PV systems that fall into one of two categories:

1) catastrophic, as in, the destruction of modules, strings or entire systems, e.g., modules unravel from their mounts, racks collapse, and glass shatters; and 2) sub-catastrophic, as in, visual inspection results in no detectable damage, even though internal damage may have occurred to the solar cells or other module components, Detectable only with costly imaging techniques, such as infrared (IR) or electroluminescence (EL) imaging, undiagnosed damage may deteriorate over time, resulting in accelerated performance degradation or the accelerated senescence of module components, such as backsheets and encapsulants.

In addition, the report acknowledges that technological innovation in the solar industry, including the proliferation of new materials and components, introduces uncertainty in a world of intensifying climatic stressors. The long-term reliability of emerging cell and module architectures is largely unknown, especially under extreme-weather conditions where modules and hardware components are subjected to combined and cyclic forces not captured by accelerated testing.

Moreover, the resilience of a PV system during extreme weather depends heavily on the unique characteristics of each storm — including the number and types of stressors, how these stressors interact in predictable and unpredictable ways, and how such interactions affect the system's components. Even so, generalizations around best practices can be made: 1) site planning should always include a review of weather threats specific to the site; and 2) design and procurement decisions should be based on the threat landscape. In hail-prone regions, for example, modules with thicker front glass are preferred; in snowy regions, frameless outperform framed modules; in regions where tropical cyclones are the primary risk, consideration must be paid not only to the module architecture but even more to the fasteners and other hardware that hold the system together. Stow algorithms for single-axis trackers should also be validated via tracked records of damage prevention. In addition, each site must have a set of protocols and response strategies specific to the weather threat and be prepared to follow them on short notice. And last, but not least, the operational status of a plant must be

considered. Sites under construction are more prone to erosion because ground cover is lacking, to wind damages because modules may not be properly fastened and are susceptible to flying debris, and to electrical damages, if cable and connectors are exposed to moisture. In contrast, fully operational plants are at risk of onsite fires from damages to the electrical network and may have prolonged power losses.

Key Takeaways

1. Most PV plants can survive most extreme weather events, if appropriately sited, designed and maintained.

2. This report considers weather events that 1) have short-term impacts and occur sporadically, e.g., tropical cyclones, convective storms (including hail) and 2) those that have longer-term impacts and tend to be repetitive, e.g., snow, dust storms, heatwaves, and wildfires. From an impact perspective, two types of damage can be identified in PV systems: acute and chronic. Risk assessment for PV plants in the first category is a critical first step, whereas design optimization for plants in the second is the priority. From a resilience and mitigation standpoint, site planning is essential. Risk assessment based on a review of historical weather data and the probability of future extreme weather events for each location is crucial and must be addressed in the design phase. Once the threat landscape has been properly assessed, project developers, and owners must make informed design and procurement choices. All materials and structural components must be code-compliant; module architecture also matters, as in, modules specifically designed for hail resilience. In addition, review of the racking/tracking design, including hardware, by an independent engineer is strongly encouraged. In addition, architects should pay close attention to the terrain and geological conditions at the proposed site. For example, when installing a PV system on sloped ground, the foundation should include features to prevent landslides triggered by tropical cyclones or flooding.
3. Site owners and operators should keep relevant commissioning documents, particularly those related to energy production in order to have a baseline against which future performance can be compared. Similarly, any electroluminescent (EL) and infrared (IR) images, along with records of visual inspections and I-V measurements, should be preserved.
4. Electrical performance data are essential for evaluating the effects of extreme weather events and any resulting acceleration in system degradation. When combined with weather data—such as temperature, solar irradiation, and wind speed—this information forms time-series data that can help detect weather-related damage. Awareness among site owners and maintenance teams needs to increase regarding the importance of collecting and preserving these data.
5. Robust operation and maintenance (O&M) protocols are essential. Defects left unresolved after storm exposure may worsen over time when exposed to additional environmental stressors like heat, wind, and moisture. Continuous monitoring of power output from restored PV systems is therefore critical to ensure their performance and reliability. If a significant drop in power generation is detected, the collected data will help the owner make informed decisions about further actions, such as system refurbishment.
6. Proactive maintenance is equally important and should be tailored to the probability of risk. Before a tropical cyclone, for example, tasks such as checking the t tightness of

fasteners and clearing debris, which could become airborne—should be carried out in advance.

7. If damage from extreme weather does occur, corrective maintenance should be implemented as soon as possible. Immediate steps include 1) ensuring the safety of the site by disconnecting it from the grid and opening all breakers; and 2) conducting electrical and mechanical inspections of the affected PV system. Damaged equipment should be left in situ, pending insurance or other claim-related inspections but all damaged PV modules and electrical components must be replaced prior to re-energization.

1 INTRODUCTION

Extreme weather events are defined in multiple ways: by their economic impact, probability of recurrence, intensity relative to historic measurements and distance from the mean. The Intergovernmental Panel on Climate Change (IPCC) defines extreme weather as events that are 'rare at a particular place and time of year'. The term "rare event" typically refers to an occurrence that would fall at or beyond the 10th or 90th percentile of a probability distribution derived from previous observations [1]. Additionally, the IPCC has reported that human-induced climate change is contributing to the increased intensity and frequency of most extreme weather categories, with widespread adverse impacts beyond what would occur through natural climate variability (see Figure 1).

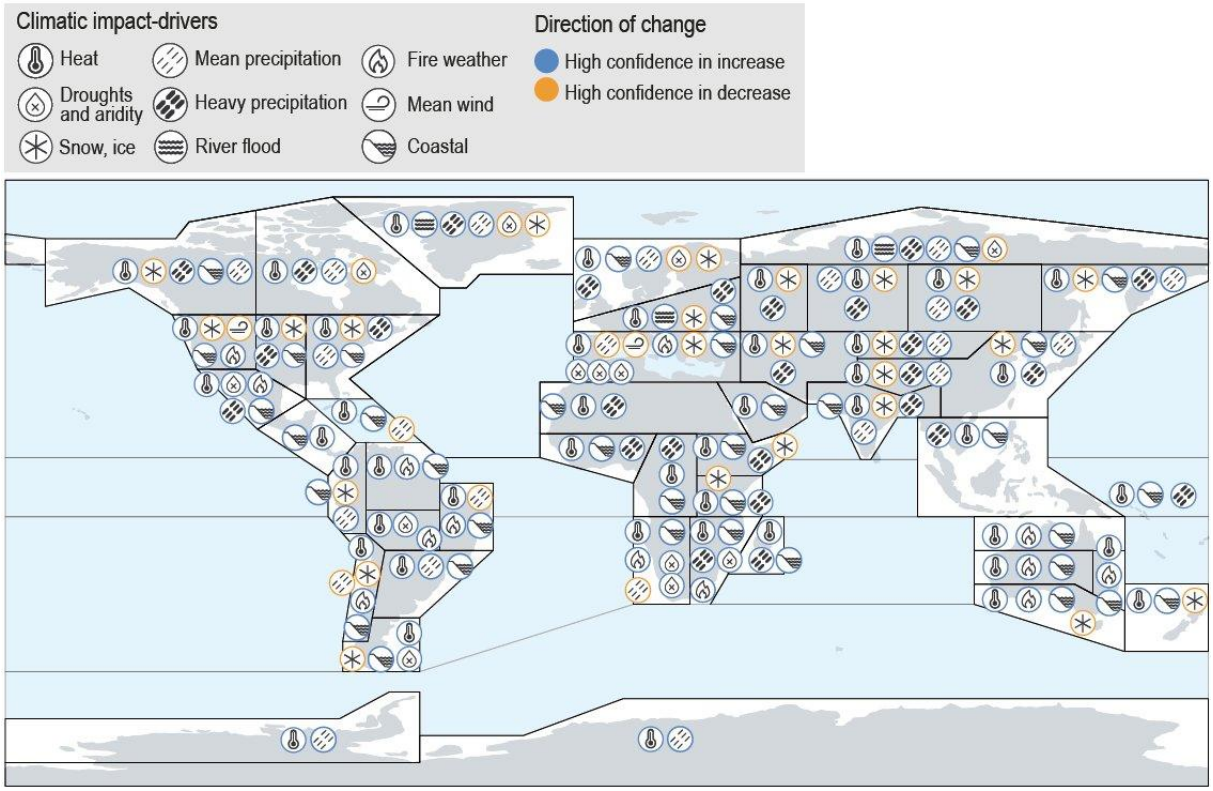

Figure 1: Projected changes in the frequency of global storm activity, determined by the IPCC Working Group 1, with blue circles indicating increases in activity and orange circles indicating a decrease. The predicted global increase in temperatures, along with increased precipitation, has a direct impact on the efficiency and reliability of PV systems [1].

The projected increase in frequency and intensity of storms has implications for PV capacity worldwide, with consequences that include 1) acute impacts (lost generation and physical destruction) and 2) chronic impacts (accelerated degradation of components and systems). Each impact category has its own key performance indicators, which range from resource availability to dollars invested in mitigation and O&M strategies, to indirect costs, including insurance premiums.

As installed global solar capacity continues to expand beyond its current 2 TW to an anticipated 8 TW by 2030, the operational and economic consequences of extreme weather are also likely to increase. The latter reflects the rapid growth in solar capacity in densely populated coastal

areas, where storm activity is high and storm-inflicted damages are likely to have a disproportionate impact on resource availability [2].

Damages to PV systems caused by tropical cyclones, heavy snowfall, hail, wildfires, and other events directly affect the levelized-cost of energy (LCOE) of PV systems (see Figure 2); they also have a broader social impact by reducing the availability of the solar generation and creating a stage for possible—even if unwarranted--social pushback [2].

Despite several highly visible case studies the multiple of impacts of weather damages on a global scale have not been comprehensively assessed. Additionally, the long-term impacts on the LCOE and performance of PV systems are not well quantified. While understanding the latter will require more information-sharing on the part of asset owners, this report captures what is known to date, with the intent of sharing best practices and helping improve the resilience of PV systems worldwide.

In this report, the authors, a cohort of PV experts distributed across five continents, examine seven types of extreme weather events that occur globally and present them in the following order: tropical cyclones, convective storms, snowstorms, dust storms, heat waves, floods, and wildfires. For each extreme weather event we strive to capture—depending on available data—impacts during the acute phase (e.g., power generation reduction due to irradiance loss and PV system damage from mechanical stress) as well as during the chronic phase (e.g., latent reliability issues in PV modules and balance of system components, leading to underperformance). It is also important to note that damage to PV systems can occur during construction or once the plant is fully operational. The construction phase poses unique challenges: sites may be graded but generally lack ground cover and are therefore highly vulnerable to flooding and erosion; modules may be on racks but not inter-connected and not torque-verified; connectors may be unmated and uncapped, and therefore exposed to moisture and dust, and cables may lie in open trenches.

This report also acknowledges underlying trends in the PV industry that are contributing to the increase in storm-related damages, including the shortage of skilled installers and the proliferation of larger and thinner modules. Our intent is not to imply that PV systems are inherently vulnerable to extreme weather but rather to provide an evidence-based rationale for designing more robust systems, a strategic approach tailored to specific weather threats. In addition, we address mitigation strategies, including both predictive and corrective maintenance approaches, to improve overall system resilience. Readers should note that general principles of resilience apply to multiple storm categories and will find certain mitigation strategies repeated in multiple chapters. The overlap is intentional, enabling each chapter to stand on its own.

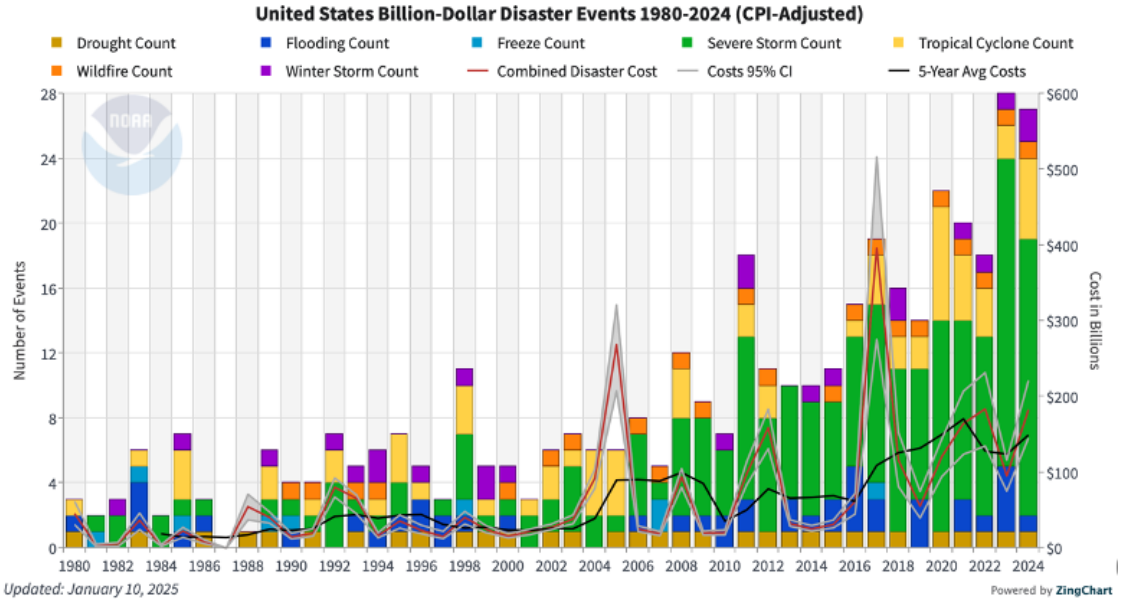

Figure 2: U.S. disaster cost assessments of the total, direct losses ($) inflicted by: tropical cyclones, inland floods, drought & heat waves, severe local storms (i.e., tornado, hail, straight-line wind damage), wildfires, crop freeze events and winter storms [3].

2 TROPICAL CYCLONES: HURRICANES, TYPHOONS AND MONSOONS

2.1 Overview

Tropical cyclone is a generic term encompassing hurricanes, typhoons, and cyclones. These destructive weather events are trans-global, occurring along the eastern and western coasts of North America, and in Asia (i.e., the Indian Ocean and the West Pacific Ocean), as shown in Figure 3 [4]. While the specific definitions, including intensity, of each type of tropical cyclone vary, they can cause severe damage to infrastructure, including homes, electrical lines and transportation networks, due to their high winds (generally exceeding 33 m/s ≃ 119 km/h) and heavy rainfall (which can lead to flooding). In recent years, PV systems located in the path of tropical cyclones have also seen catastrophic damage, prompting efforts to identify resilient designs and best practices for plant survivability.

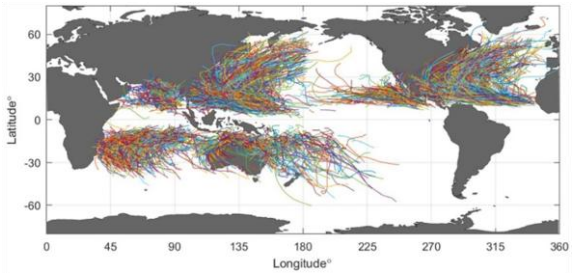

Figure 3: Tracks of tropical cyclones extracted from IBTrACS [4]. Creative Commons License CC BY 4.0.

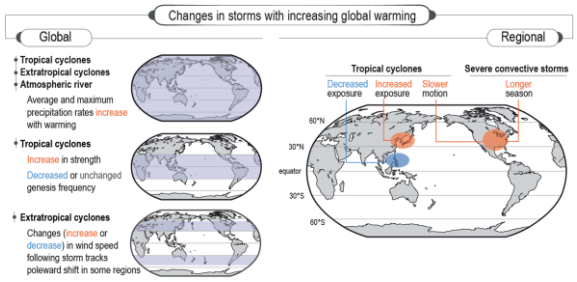

Figure 4: Summary schematic of past and projected changes in tropical cyclone behaviour [1].

According to IPCC projections (see Figure 4), the intensity of tropical cyclones is expected to increase, although the frequency of their formation may decrease or remain unchanged [1]. One indicator of their projected intensity is a proposed extension to the Saffir-Simpson hurricane scale, from Category 5 (over 70 m/s = 252 km/h), to Category 6 for wind speeds exceeding 86 m/s (≃ 310 km/h) [5]. Moreover, because tropical cyclones are temperature-dependent (related to rising ocean temperatures) an increase in Category 6-equivalent storms, commensurate with the level of global warming can be expected

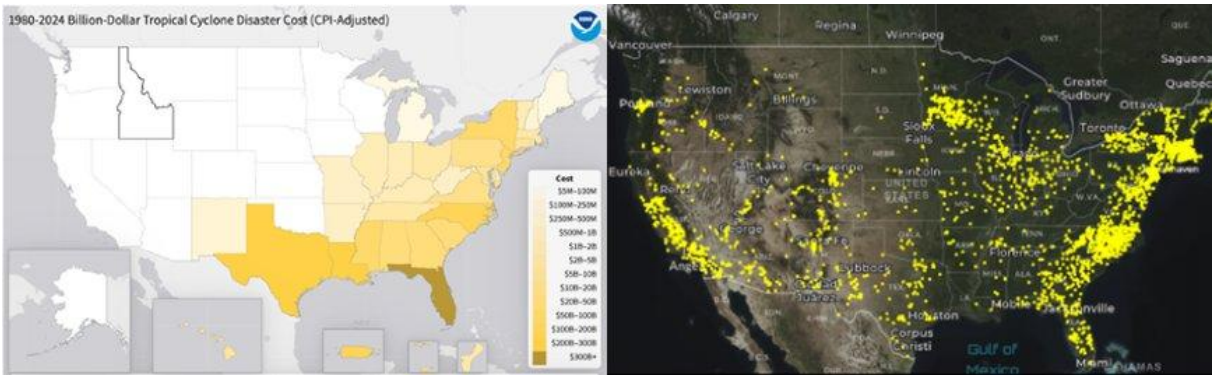

Figure 5: Image (left) depicts economic damages >$1B USD attributable to tropical cyclones [6]; image (right) shows the distribution of PV power plants [7], [8]. Florida, which has had the largest number of tropical cyclone disasters in US, ranks third in solar capacity; Texas ranks second in both categories.

PV systems installed in coastal areas in North America and Asia are considered most at risk from tropical cyclones [1], [5], as seen in Figure 5. Furthermore, as storm activity expands, regions previously unaffected by intense storms may be at risk, exemplified by Hurricane Helene, which in 2024 devasted an area of North Carolina more than 500 miles (≃ 805 km) inland.

2.2 Equipment damage and failure mechanisms

Storm damages are generally attributable to poorly designed racking systems and/or poorly installed bolts and fasteners. Fasteners that are inadequately torqued or not designed for high-stress conditions (as in having low mechanical strength) are a common problem. Fretting and the resultant wear of threaded bolts can lead to loosening during wind events—and if the wind load is severe enough—cause cascading effects that range from the collapse of the racking or tracker platform to modules being ripped from their fasteners, often in multiples (see Figure 6). In addition, excessive, repetitive wind loads can lead to irreversible deformation of both fasteners and support structures if they exceed the allowable stress of the mounting hardware.

Figure 6: Tracker system damaged by Hurricane Helene in the US in 2024 is shown here. Fastener failures caused modules to detach from the torque tube and tear from electrical connections.

Tracking systems, where modules are attached to a single torque tube fixed on one end, are vulnerable to torsional stress that is exacerbated by high wind loading on the modules. If the hardware is insufficient for the wind load, strong winds can induce torsional galloping, creating escalating stress on the modules, resulting in a runaway-failure event. The process begins when the end-of-row modules begin to flutter and then twist inward from the edges toward the central modules, which are supported by the drive mechanism and are therefore the most rigid part of the row. As the outer modules loosen, the twisting gradually intensifies, spreading from one module to another. Eventually, the tracker will twist apart, resulting in airborne modules and the loss of the entire row [9].

Damage may also extend beyond mechanical failures to include a heightened risk of electrical failure. High winds can loosen cables, causing fretting within connectors and/or partial separation of the pin and socket. Loose or poorly torqued connectors then become vulnerable to moisture penetration, which in turn leads to corrosion, high resistance and ultimately failure [10]. Heavy rainfall can also lead to water penetration inside the housing of combiner boxes/power conditioner boxes, disrupting the electrical circuitry throughout a plant.

2.3 Economic impacts

The economic impacts of tropical cyclones on PV plants are manifold, ranging from lost generation to physical damages to increased operating expenses. One study of generation losses during 18 hurricane events, showed power losses of approximately 50% during the period of storm activity (likely attributable to a combination of trackers in stow position and reduced irradiance), although generation returned to normal afterwards [11]. Statistical analysis also revealed that the performance ratio during hurricane days was—as might be expected—12.6%

lower than on non-hurricane days [12]. Recent data, however, suggests that annual production losses (median values) due to high winds and heavy rain are relatively small, around 1% for each category [13]. The same study suggests that degradation rates for PV systems accelerate for sites which exceed a minimum wind speed threshold (25 m/s = 90 km/h) [13]. As explained by the authors, this effect may vary depending on the surrounding environment (e.g., wind shadowing) and/or appropriate operation and maintenance practices. While more data is needed, it appears feasible to predict generation losses due to tropical cyclones and incorporate those predictive models into the design and procurement stages for new plants to ensure more accurate LCOE calculations and provide a justification for more robust designs.

Such probability modelling is increasingly justifiable based on the escalating frequency and rising costs of storm events. As the number of PV installations grows, insurance payouts for severe-weather damage are likely to rise. In Japan, for example, insurance payouts increased by a factor of 3.7 from 2017 to 2021 [14], with a significant portion attributed to damages from high winds, flooding, and related causes [15]. Much as the intensity of tropical cyclones is expected to increase [1], insurance rates for PV systems are also likely to rise, commensurate with the heightened risk of severe damage. This represents an indirect, but measurable, economic impact of extreme weather.

2.4 Diagnostic tools

Two types of post-storm assessments are needed to a diagnose the damage caused by tropical cyclones: 1) an electrical analysis to accurately estimate the storm's impacts on electrical safety and power production; and 2) a structural analysis to document any physical damages to modules, racking and associated hardware. Daily or real-time monitoring of PV electrical systems in areas prone to tropical cyclones is highly advisable and various service providers offer monitoring systems with advanced technologies (e.g., their own PV performance software). If a properly monitored PV system shows an abnormal reduction in electrical generation during or after a tropical cyclone, electrical safety must be promptly confirmed. In particular, combiner boxes, inverters and high-voltage equipment enclosures should be checked for ingress of wind-driven rain. Drone-mounted or handheld thermal cameras can also be deployed to verify the electrical safety of PV connectors. Less urgent from a safety perspective is the diagnosis of damage to the solar cells in the absence of broken module glass. The latter involves subjecting a subset of modules to EL-imaging but the process is time-consuming and expensive and generally undertaken only if there is reason to suspect cell damage, and—even then—may involve only a sampling of modules (for more information on EL imaging, see Chapter 3).

Figure 7: Ground-level robots, equipped with thermal and optical cameras can image front and rear-sides of the modules, as well as the rear-side electrical network. Photo: *L. Burnham.*

In addition to employing aerial drones to survey the site and document site-wide damages (e.g., number and location of damaged modules/rows), manual inspections are needed to

ascertain structural damage. Although Light Detection and Ranging (LiDAR) technology (with or without an unmanned aerial vehicle) could be valuable in the future [16], best practices today call for a detailed row-by-row inspection to assess the integrity of the modules, racking hardware and electrical BoS. Ground-level robots that survey each module and take thermal images of the connectors, are a technology that is gaining interest, especially for the largest PV plants, (see Figure 7) but have yet to become commonplace. New-generation drones that can fly between the rows and also capture backside images are also attracting interest but require more sophisticated controls and navigation software.

2.5 Mitigation strategies

Because PV installations are proliferating in tropical and sub-tropical regions, damages to PV systems from tropical cyclones are on the rise. To mitigate the escalating threat posed by severe winds and heavy rain, best practices (summarized in Table 1) can be categorized into four stages as follows: 1) project planning, 2) system design, 3) construction and commissioning, 4) operation and maintenance.

In the *project planning stage*, it is important to consider the historic patterns of tropical cyclone activity (see Table 2). This information is crucial for determining whether a specific location is high or low risk for a catastrophic storm and whether or not a resilient PV system can be designed for that site. For example, one can estimate both the capital expenditure (CAPEX) and operational expenditure (OPEX) for a proposed PV system based on the relevant meteorological parameters, e.g., wind speed, precipitation, etc. Analysis of historical wind patterns is also advised because predominant wind direction as well as its ramp rate can inform tracker stow strategies.

The *design phase*, however, is the crucial stage for mitigating serious damage [17]. Detailed design recommendations for PV systems installed in cyclone-prone areas are shown in Table 3. System designers should adhere to these guidelines to ensure that materials for structural components and PV modules are chosen within the specified limits set by these regulations. In addition, the recommendations described in the chapter 5.6.5 of “Guidelines for Operation and Maintenance of Photovoltaic Power Plants in Different Climates” should be considered [10]. The authors of this report also strongly recommend that the choice of a racking/tracking system be reviewed by an independent engineer, with expertise in bolted joints and failure mechanisms specific to climatic stressors.

During *construction and commissioning,* installation training is paramount, and field crews should be explicitly trained to properly install module fasteners as well as bolted joints, which are widely acknowledged to be the weak point in many racking systems and insufficiently covered by existing codes and standards. For example, current PV auditing standards, such as IEC 62446, do not include checks for fasteners or torque audits despite their importance to system reliability. At the commissioning stage, the agent of record should (1) verify the correct installation of all—or a significant subset of—designated structural connections, and (2) conduct torque audits on at least 1% of the fasteners. If 10% or more of these fasteners are either over-tightened or under-tightened, the contractor should reinstall all fasteners [18]. In addition, the improper management of electrical cables poses significant risks to the integrity of the PV connectors and ultimately the electrical balance-of-systems. Other poor practices that should be avoided include loose hanging wires, widespread reliance on plastic cable ties, and improper routing of PV wires [19].

During the *O&M* stage, the site-owner or site-operator should implement clear protocols for pre- and post-storm O&M tasks, including stow strategies for tracking systems in advance of a storm and post-storm inspections that include module examinations, torque tests of fasteners

and thermal imaging of connectors [20]. While these tasks can be performed by onsite personnel, hiring skilled consulting engineers to manage the recovery efforts is recommended. In addition, safety checks conducted by a qualified electrician are essential before accessing the system [20].

2.6 Key takeaways and recommendations

In regions prone to frequent cyclones, project planning should include an overall risk assessment, accounting for historical and predicted weather patterns as well as design and procurement decisions. In plain words, historical weather conditions, as well as future projections, should inform the planning stage and be reflected in each specific site design.

Pre- and post-storm planning for existing, as well as partially constructed, PV systems, is also of high importance. Such planning includes both installation and response training for onsite crews and the dissemination of detailed protocols to minimize confusion and maximize both response and recovery strategies. A rapidly executed pre-storm response — in accordance with the weather forecast and alarms reported by various agents (Table 2) — should be integral to any onsite operations manual. The following countermeasures are minimum requirements.

Pre-storm phase for systems under construction:

- Clear debris and secure loose materials in and around arrays to avoid wind-blown objects that can damage modules.
- Make sure all exposed connectors are capped or—at a minimum—fastened under the modules, where their exposure to water and dust ingress is minimized.
- Secure cables to the racking to avoid abrasion and stress from wind loading.

Pre-storm phase for commissioned systems:

- Conduct a torque audit on all fasteners.
- Stow single-axis tracker systems per manufacturer specifications.
- Power down all components by opening breakers, fuses, and switches.

Post-storm phase for systems under construction (in addition to the recommendations for commissioned systems):

- Inspect racking posts for shifting or loosening that may have been caused by erosion.
- Document any flooding of open trenches and exposed cables.
- Check integrity of module pallets.
- Replace any open, unmated, connectors that appear to be dirty or wet.

Post-storm phase for commissioned systems:

- Visually inspect damages to PV modules (front and back), mounting structures, fasteners, cables, connectors (module-to-module and homerun), combiner boxes, inverter boxes, wiring, and other components. It is important to 1) check purlins and rails for evidence of cracks or deformation; 2) look for evidence of cable abrasion; 3) replace broken zip ties and other failed cable fasteners; and 4) verify that connectors are not sitting in pooled water or show evidence of submersion (e.g., algal growth).
- Dry and clean the interiors of combiner boxes and inverter boxes. Components inboxes that were exposed to water or high humidity should be closely inspected for indicators of moisture ingress, replaced if necessary, and thereafter monitored for evidence of increased resistance to ensure electrical safety.

- Perform torque audits on fasteners.
- Test for electrical faults in all systems.
- Replace any damaged electrical components before energizing the system.
- Subject subset of connectors to thermal imaging after the system has been re-energized and at 6 and 12 months.

Table 1: References that include recommendations for reducing damages from tropical cyclones.

Country	Issuer	Title	Issued Year	Ref #
USA	US-FEMA	Hurricanes Irma and Maria in The U.S. Virgin Islands - Building Performance Observations, Recommendations, and Technical Guidance	2018	[21]
USA	US-FEMA	Rooftop Solar Panel Attachment: Design, Installation, and Maintenance - Hurricanes Irma and Maria in the U.S. Virgin Islands - Recovery Advisory	2018	[22]
USA	US-FEMP	Solar Photovoltaic Systems in Hurricanes and Other Severe Weather	2018	[23]
USA	RMI	Solar Under Storm: Select Best Practices for Resilient Ground-Mount PV Systems with Hurricane Exposure	2018	[24]
USA	NREL	Solar Photovoltaics in Severe Weather: Cost Considerations for Storm Hardening PV Systems for Resilience	2020	[25]
USA	RMI	Solar Under Storm Part II: Select Best Practices for Resilient Roof-Mount PV Systems with Hurricane Exposure	2020	[26]
USA	RMI	Solar Under Storm for Policymakers: Select Best Practices for Resilient Photovoltaic Systems for Small Island Developing States	2020	[27]
USA	US-FEMP	PV System Owner's Guide to Identifying, Assessing, and Addressing Weather Vulnerabilities, Risks, and Impacts	2021	[19]
USA	NREL	Preparing Solar Photovoltaic Systems against Storms	2022	[20]
USA	US-FEMP	Toward Solar Photovoltaic Storm Resilience - Learning from Hurricane Loss and Rebuilding Better	2023	[18]
AUS	Queensland Gov.	Cyclone and Storm Tide Resilient Building Guidance for Queensland Homes	2019	[28]
	Nextracker	Mitigating Extreme Weather Risk Part 1: Understanding How Differentiated Design and Control Strategies Unlock New Opportunities for Solar Development	2020	[29]
	Nextracker	Mitigating Extreme Weather Risk Part 2: Surviving High-Wind Events and Dynamic-Wind Effects with Differentiated Solar Project Design and Control Strategies	2021	[30]
	FM Global	Property Loss Prevention Data Sheets 1-15: Roof-Mounted Solar Photovoltaic Panels	2024	[31]
	FM Global	Property Loss Prevention Data Sheets 7-106: Ground-Mounted Solar Photovoltaic Power	2024	[32]

Table 2: Official information sources on tropical cyclones in each region.

Area	Official Information Source
North Atlantic, Eastern- and Central-Pacific	United States National Hurricane Center
Western Pacific	Japan Meteorological Agency
Indian Ocean	India Meteorological Department
South Indian Ocean from 30°E to 90°E	Météo-France – La Reunion
South Indian Ocean from 90°E to 125°E, north of 10°S	Indonesian BMKG
South Indian Ocean and South Pacific Ocean from 90°E to 160°E	Australian Bureau of Meteorology
South Pacific east of 160°E, north of 10°S	Papua New Guinea National Weather Service
South Pacific west of 160°E, north of 25° S	Fiji Meteorological Service
South Pacific west of 160°E, south of 25°S	MetService New Zealand

Table 3: Representative regulations and guidelines for wind load design for PV systems.

Country / Region	Issuer	Code #	Title	Issued Year	Ref #
USA	ASCE	7-22	Minimum Design Loads and Associated Criteria for Buildings and Other Structures	2021	[33]
USA	SEAOC	PV2-2017	Wind Design for Solar Arrays	2017	[34]
EU	CEN	EN 1991-1-4/AC	Eurocode 1: Actions on Structures - Part 1-4: General Actions - Wind Actions	2010	[35]
AU/NZ	SA/NZS	AS/NZS 1170.2	Structural Design Actions, Part 2: Wind Actions	2021	[36]
CN	CS	GB 50009-2012	Load Code for The Design of Building Structures	2012	[37]
TW	CNS-TW	CNS 16189	Evaluation Guide for Design Wind Loads of Photovoltaic Systems	2022	[38]
JP	METI		Interpretation for "Ministerial Order on Technical Standards for Solar Photovoltaic Power Generation Facilities"	2021	[39]
JP	JISC	JIS C 8955	Load Design Guide on Structures for Photovoltaic Array	2017	[40]
JP	NEDO		Design Guidelines for Ground-Mounted Solar Photovoltaic Power Systems	2019	[41]
JP	NEDO		Design and Construction Guidelines for Sloped-Terrestrial Mounted Solar Photovoltaic Power Systems	2023	[42]
JP	NEDO		Design and Construction Guidelines for Floating Solar Photovoltaic Power Systems	2023	[43]
JP	NEDO		Design and Construction Guidelines for Agrivoltaic Systems	2023	[44]
	IEC	IEC TS 63348	Evaluation of Photovoltaic (PV) Module to Mounting Structure Interface	under discussion	[45]

3 SEVERE CONVECTIVE STORMS: HAIL, TORNADOES AND STRAIGHT-LINE WINDS

3.1 Overview

Severe convective storms (e.g., severe thunderstorms) produce damaging hail, intense wind gusts, and tornadoes that can result in significant property losses [46]. In recent years, severe hail, while relatively infrequent, has emerged as the leading cause of insured losses to PV power systems and therefore a leading concern for the solar industry [47]. This chapter emphasizes hail risk identification, quantification, and mitigation to align with published insurance loss data but the general analytical and scientific principles—and engineering-based risk assessment methodologies—presented here are applicable to all convective storm perils, including tornadoes and straight-line winds.

3.1.1 Definitions

The U.S. National Weather Service (NWS) glossary [48], maintained by the National Oceanic and Atmospheric Administration (NOAA), provides meteorological definitions, including those summarized below, that are foundational to an understanding of severe convective storm risk:

Severe thunderstorm. A thunderstorm that produces a tornado, with winds of at least 26 m/s (=93 km/h), and/or hail with a diameter of more than 25 mm.

Hail. Showery precipitation in the form of irregular pellets or balls of ice more than 5 mm in diameter. S*evere hail*, as defined by the NWS, has a diameter of more than 25 mm.

Tornado. A violently rotating column of air with circulation reaching the ground; on a local scale, tornadoes are the most destructive atmospheric phenomenon.

Straight-line winds. Thunderstorm winds that have no rotation (i.e., not a tornado).

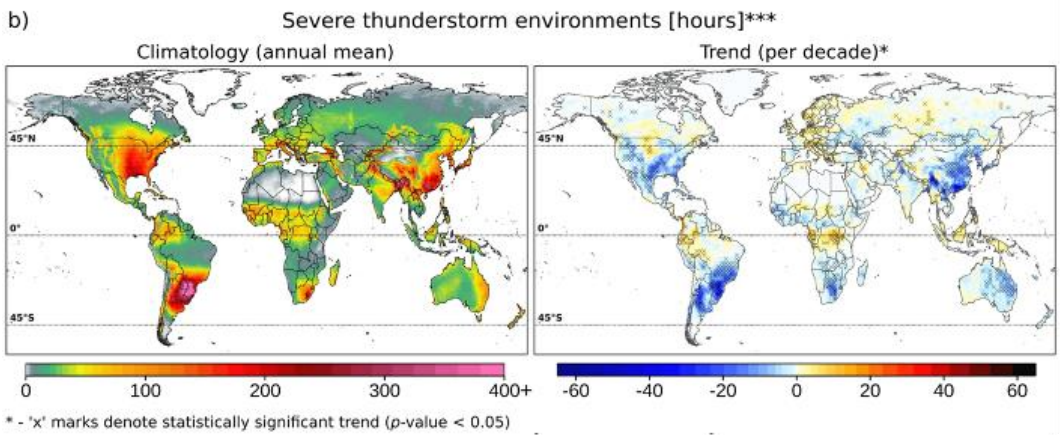

Figure 8: European Centre for Medium-Range Weather Forecasts (ECMWF) Reanalysis v5 (ERA5) depicts climatology and trends data for severe thunderstorm environments [49].

3.1.2 Geographic distribution

Convective storms are a global phenomenon and common in locations seeing significant solar market growth (e.g., central United States, southern Europe, southern China, and eastern

Australia) and are coincident with the severe thunderstorm environments shown in Figure 8 [49]. Though far smaller in scale than hurricanes and typhoons (see Chapter 2), severe convective storms occur worldwide and pose a threat on every continent except Antarctica [46]. Because of their ubiquitous geographic distribution, severe convective storms are potentially more damaging to solar assets than any other large-scale natural catastrophes on an annual basis [47] Hailstones associated with thunderstorms occur in many locations at a rate of more than one event per year, a far greater frequency than the occurrence of tornadoes [50].

Moreover, climate [51] models generally predict that meteorological conditions conducive to thunderstorms will intensify in future decades, resulting in an increase in storm frequency and severity [51]. Details about how this projected increase plays out both regionally and on a global scale, however, are the subject of much scientific study [49]. While the scientific community's understanding of severe convective storm climatology and trends remains a work in progress [49],[51], the insurance industry has amassed extensive data on the financial impacts of smaller-scale severe weather events (e.g., hail, windstorms, and tornadoes), suggesting an expanding threat landscape. A 2019 study supported by Munich Re, for example, documented a significant increase in hail events in southern Europe over a 37-year period [52]. More recently, GCube Insurance reported that over a five-year period (2018–2023), hail resulting from severe convective storms accounted for 54% of total insured solar sector losses [53].

3.2 Case studies, failure modes, and event severity

The following case studies characterize the frequency, severity, and technical considerations specifically associated with hailstorms or windstorms, including damages (see Figure 9).

3.2.1 Hailstorm loss events

Hail forms via accretion when convective storm updrafts carry water droplets into extremely cold areas of the atmosphere, where they freeze, grow, and increase in mass. Hail falls when the downward gravitational force exceeds the strength of the thunderstorm updraft [54]. To meet the minimum ballistic-impact requirements in the IEC 61215-2 product qualification standard, PV module designs must withstand 11 impacts of a 25-mm ice ball at terminal velocity. As solar markets have proliferated globally, so have reports of catastrophic damage consistent with naturally occurring hail having a diameter of more than 25 mm. The following case studies illustrate the range of impacts hail can have on PV systems globally.

Noord-Brabant/Limburg, Netherlands (2016). On June 23, 2016, heavy thunderstorms in the southeast of the Netherlands produced severe hail and property damage. Local reports documented maximum hailstone diameters in the 6 cm (tennis ball) to 7 cm (baseball) range. A comprehensive statistical analysis of the resulting insured losses noted that visible damage to solar panels was surprisingly most pronounced in areas exposed to hail in the 4 cm (ping-pong ball) to 5 cm (larger than a golf ball) range, based on the frequency and distribution of hail in this size range [55]. In addition to visible hail damage, the study also noted insured losses associated with "invisible" hail damage (cell cracks) to solar modules. In a typical year, hail

Figure 9: Solar array in Colorado damaged by a record hailstorm that impacted 25–50% of the on-site PV modules. Photo: *Dennis Schroeder* / NREL.

accounts for 19% of insured severe weather losses in the Netherlands; in 2016, hail accounted for 73% of severe weather-related insured damage.

Pecos County, Texas, United States (2019). In May 2019, seasonal thunderstorms in West Texas produced damaging hail that fell on the 182 MW-rated Midway Solar farm. According to insurance reports, severe hail damaged more than 400,000 solar modules at the 600-hectare site, resulting in insured losses of $70 million to $80 million [56]. Hail damages included broken glass as well as modules with cracked cells [57]. In response to the historic magnitude of these losses, insurance premiums increased by as much as 400% in this region [58].

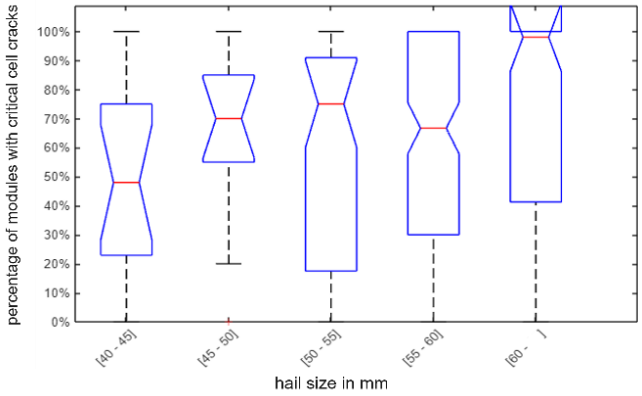

Figure 10: Percentage of modules with critical cell cracks as a function of hailstone diameter [60].

Switzerland (2021). During June and July 2021, Switzerland experienced a series of widespread and intense hailstorms, the most severe of which occurred on June 28th. Hailstones reached sizes of up to 9 cm, causing significant damage in densely populated areas, resulting in some of the most expensive hail-related losses in recent decades [59]. Approximately 15% of all PV systems in Switzerland were situated in areas that experienced hailstones larger than 5 cm. Damages are typically expected when hailstones exceed 4 cm, with a significant increase in damage observed from hail above 5 cm in diameter. In addition to glass breakage, EL images of approximately 6,000 modules from 411 affected PV systems revealed significant cell cracks in 57% of the modules. The likelihood of cell cracks increases with hail size, but the spread for all categories is high (see Figure 10) [60].

West Texas, United States (2022). The hail season in Texas (May–June) brought devastation to multiple solar projects, with cumulative hail damages estimates at $300 million [61]. According to insurance reports, four separate solar farms (347 MW, 415 MW, 500 MW, 500 MW) located in three counties (Andrews, Brown, and Pecos) incurred significant hail damages, with damaging hail sizes across these sites ranging from 6 cm (tennis ball) to 9 cm (softball) [57].

3.2.2 Windstorm loss events

Convective storm-induced wind damage typically results from straight-line winds rather than tornadoes. Though tornado wind speeds may reach 160 to 480 km/h (ca. 44 to 133 m/s) and will destroy any PV systems in their path, tornadoes are typically small-scale, short-lived, and infrequent events. By comparison, straight-line winds in the 80 to 100 km/h (22 to 28 m/s) range—notably lower than typical project design wind speeds—have inflicted damage on multiple fixed-tilt and single-axis tracker systems. In fact, as early as 2015, an engineering report noted that while structural wind damage is rare in utility-scale applications, failures have been observed in code-compliant structures [62]; a finding that has been reinforced anecdotally. Based on reports of helical twisting in fielded systems, wind engineers posit that torsional instability in single-axis trackers, combined with improperly designed or torqued hardware, could be the root cause of observed failures [63]. Case studies from Australia and the US illustrate the damages to PV from windstorms.

Darling Downs, Queensland, Australia (2018). In October 2018, a seasonal thunderstorm damaged single-axis trackers supporting approximately 2,000 solar modules at the 55 MW-

rated Oakey 2 solar project [30]. Though recorded wind gusts associated with the convective storm peaked at only 74 km/h (≃ 21 m/s), the two-up, module-in-portrait-orientation trackers sustained structural damages consistent with torsional galloping, a wind-induced instability that can occur in flexible structures at relatively modest wind speeds [9].

Lamar County, Texas, United States (2023). In March 2023, a utility-scale solar project in northern Texas, also the same module design as Darling Downs, incurred straight-line wind damages consistent with torsional tracker instability. According to insurance industry stakeholders, the site experienced maximum wind gusts in the 80 km/h (≃ 22 m/s) range, well below the project design wind speed, resulting in damages estimated at $30 million [56].

3.3 Economic impacts of convective storm damage

Severe hail is the leading cause of financial losses for the solar industry, worldwide. Though hail-related insurance claims are relatively infrequent, hail damages are far more costly than those associated with other types of claims. As an example, GCube's solar-loss data for 2018–2023 shows hail accounting for 1.4% of claims volume (i.e., the total number of claims), but 54.2% of claims value (i.e., total incurred costs) [53]. Within this dataset, the four largest claims, which together account for more than $224 million in losses, were /attributed to hail. By comparison, the combined losses due to all other types of severe weather events—including thunderstorms, floods, hurricanes, wind events, and lightning—accounted for less than 10% of GCube's total incurred losses [53].

Direct economic impacts, which are not exclusive to hail, include lost energy generation, inventory and forensic investigation costs, advisory costs to determine root causes, engineering costs to address compatibility issues with replacement hardware, time and material costs for repowering, inbound and outbound shipping costs, recycling and disposal costs, legal costs arising from disputes among project stakeholders, insurance premium cost increases, and so forth. Although hail loss events are infrequent, the magnitude of the resulting damages can increase insurance rates, erode investor confidence and raise consumer concerns.

3.4 Response strategies for convective storm damage

Appropriate response strategies vary according to the capacity of the impacted PV system. In residential and commercial applications, the property owner typically initiates an insurance claim in the aftermath of a loss event. To process the claim, the insurance adjuster requires a damage estimate from a PV technical expert, such as the original installation contractor or an O&M specialist. That person inspects a site to identify visible (typically glass breakage) and invisible damages. As shown in Figure 11, invisible damages (cell cracking in the absence of glass damage) are best diagnosed via EL imaging [64], [65], but the process, which must be executed in the dark, is relatively complex and costly.. In distributed applications, therefore, technicians typically use a combination of thermal infrared (IR) imaging, I-V curve tracing, and visual inspection to identify damaged cells, but cell cracks only become visible in IR images and I-

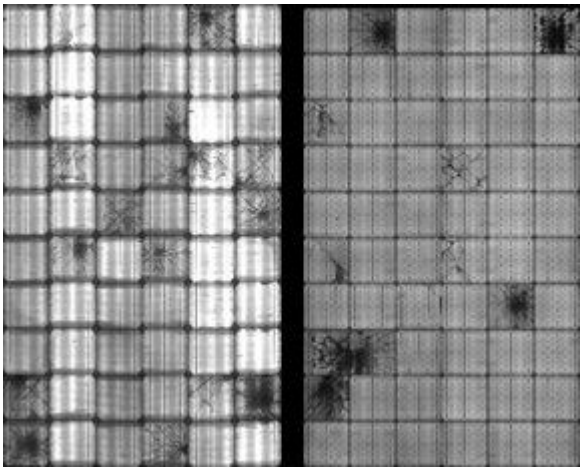

Figure 11: EL images of hail-damaged modules have distinctive crack patterns.

V curves after several years of aging. As a result, modules that may have undiagnosed cracked cells should be closely monitored in the years following a hail event.

Ideally, a rooftop system is repowered using direct replacement parts, but project stakeholders may be challenged to find modules that match the physical form and electrical characteristics of the originals. If so, service providers are typically left with two paths forward. The first option is to redesign the system to integrate new and salvaged components into parallel circuits or systems; the second option is to declare a total loss and apply the insurance payment to the purchase of a new system.

Response strategies are more complex for a hail-impacted utility-scale site and should be codified in the project's O&M contract, which should include a detailed severe convective storm response plan (e.g., a tracker stow-strategy) designed to minimize severe hail or wind damage (see Section 3.5). In addition, the on-site project manager and remote operation control centre (ROCC) personnel should have sufficient training, permissions, and access to the plant's supervisory control data acquisition (SCADA) system to quickly implement the response plan based on meteorological data. Following a loss event, the site manager or ROCC personnel should thoroughly document any evidence or activities that may be needed to support warranty and/or insurance claims [66].

Removing, recycling, and replacing 400,000 or more damaged PV modules is an expensive and logistically complex undertaking. Forensic activities typically start with a system-level aerial survey that uses photographic and IR imagery to identify broken glass (visible damage) and degraded (invisible damage) modules. Adding to the complexity is that damages can be random, indicative of the stochastic nature of a hail event, and may result in an uneven distribution of module failures, including glass breakage on the rear side only, complicating the inspection process. EL imaging is often required because it can identify the root cause of cell cracking, specifically cracks that have distinctive patterns indicative of a hail strike, but only a pre-determined percentage of modules may be imaged. Informed by the data collected, an independent engineer or technical advisor will develop a repowering plan. In large utility-scale applications (>100 MW), hail damage is typically concentrated in specific blocks or subarrays. Therefore, module-level diagnostics are generally performed on a block-by-block or row-by-row basis, according to a statistical assessment of the storm damages.

3.5 Mitigation strategies for convective storm risk

Although severe convective storm risk is inevitable in some locations, large project losses can be minimized with improved technical literacy, due diligence, and risk mitigation practices [67]. Specific strategies include the following:

Identify and quantify severe weather risks. During the siting and design phase, all prospective sites should be subjected to an initial storm risk assessment [68], [69]. The goal is to characterize hail and straight-line wind risk (low, moderate, high) on a location-specific basis. Qualified technical advisors should quantify probabilistic loss levels over the event recurrence intervals required by insurers (e.g., a 1-in-500-year event) and typical investment hold periods (e.g., a 1-in-10-, 20-, and 40-year hold). The goal of these loss studies is to provide comparative probable maximum loss (PML) and average annual loss (AAL) values based on site-specific meteorological characteristics (e.g., historical hail events, identified by both severity and

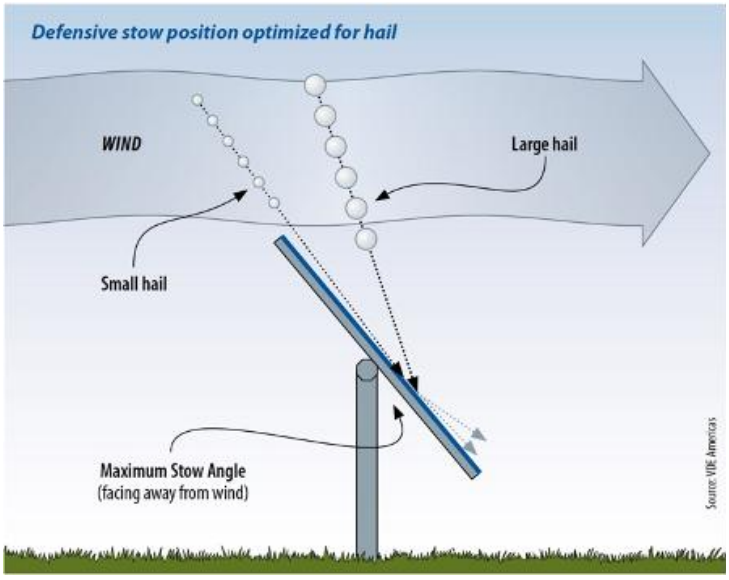

Figure 12: Single-axis tracker defensive stow position optimized for hail [67].

frequency) and project-specific technical considerations (e.g., PV module glass thickness, tracker stow angle, and so forth) [56].

Make strategic technical adaptations. Strategic design choices can greatly increase the likelihood that a PV site will withstand a hailstorm while optimizing investor returns. Project stakeholders should pay special attention to module specifications during procurement (specifically the thickness of the front glass and presence of a glass backsheet). Beyond-qualification testing has shown that module ballistic-impact resistance is a function of front glass thickness and heat strengthening [70]. Module tilt angle also contributes to hail resilience [71] and the selection of a tracker system is also key to surviving a hailstorm. The features that matter include advanced stow capabilities, rapid response times and bolted joints that can withstand high wind loading and cyclical vibration. An optimal defensive position is shown in Figure 12. In addition, because many storm gusts and downbursts are small and unevenly distributed, a site should have multiple anemometers to ensure quality windspeed data.

In high-risk locations, stakeholders can mitigate financial risk by deploying hail-resistant modules [67], [70] and adhering to hail-stow best practices [66], [71]. In some jurisdictions, enhanced hail resistance, as determined by building-material classification standards, is a building code or insurability requirement [72]. In locations exposed to damaging straight-line winds, attention should be paid to tracker wind load specifications, and the system's design (e.g., number of modules in portrait, perimeter row enhancements, dynamic wind susceptibility), tracker stow strategy, and ROCC capabilities [66].

Improve test standards and operating protocols. The ballistic-impact test requirements in IEC 61215-2 are pass/fail in nature and do not differentiate product designs based on severe hail vulnerability or resiliency [73]. Nor do these tests, which rely on ice balls, account for the uneven surface morphology of hail. Designing and deploying hail-hardened PV modules and systems cost-effectively requires enhanced product testing standards that provide statistically significant comparative test results and take into account the full system, from the diameter of the bolts to the size of the modules. Although enhanced testing (e.g., static wind tunnel tests, dynamic wind analysis, and computational fluid dynamic analyses) can prevent structural failures in code-compliant tracker designs under normal conditions, these tests are not required [74]. More important, in terms of hail resilience, is the adoption of defensive hail stow strategies for tracker systems, which–when executed properly--are known to measurably minimize wind- and/or hail-related damages [57], [30], [66], [73]. The next technological breakthrough will be advanced stow algorithms that quickly and automatically put trackers into defensive hail stow based on electronic weather alerts from a reputable weather service provider [66]. Where the tracker manufacturer allows, hail stow should take precedence over other stow modes, given the magnitude of hail loss events [57], [66].

3.6 Key takeaways

Severe convective storm risk is not an insurmountable barrier to PV deployment, but large losses in recent years suggest that more attention be paid to mitigation strategies and best practices.

- Severe convective storm risk to solar assets is increasing due to a perfect storm of market and technological change. On the technology front, PV systems are becoming more vulnerable as module manufacturers transition to larger format modules with weaker front glass. On the market front, utility-scale projects are increasing in locations exposed to damaging straight-line winds and severe hail.
- PV modules should be selected based on location risk. Ballistic-impact resistance is a function of front glass thickness and heat strengthening [70]; also whether or not the back sheet is glass or transparent polymer (the latter reduces resistance). Module packaging and cell technology can also influence resilience to cell cracking [13], [75]. Module sizes, frame, and mounting also impact probable hail losses.
- For best results, probabilistic models should include a conversion from in-laboratory freezer ice-ball impacts to in-field naturally occurring hail impacts [68], [76], so the data more accurately reflects hail's non-uniformity and strike angles.
- Single-axis trackers intelligent and proactive tracker controls that increase the tilt angle can significantly limit hail damage by reducing the exposed glass area and increasing the number of glancing (not direct) blows [57], [71].
- Timely and accurate early weather alerts are an important first line of defence against hail loss. The sooner the ROCC receives a severe weather alert, the sooner the operator or control system can send a hail stow-command. This early warning ensures that all trackers stow optimally in advance of an approaching storm [66].
- Solar irradiance is relatively low during a severe thunderstorm event, so proactive stowing has little impact on annual plant production [77]. Critical to survivability, however, is moving to a defensive stow position as early as possible [66].
- Because severe hail is a hyper-local phenomenon, traditional hail maps lack the granularity needed to characterize risk. The insurance industry generally maps hail risk across relatively large areas, such as one-degree longitude by one-degree latitude (circa 10,000 km^2). An important step to improving the accuracy of site- and technology-specific hail risk assessments is to calculate risk over a smaller grid area (see Figure 13) [68].

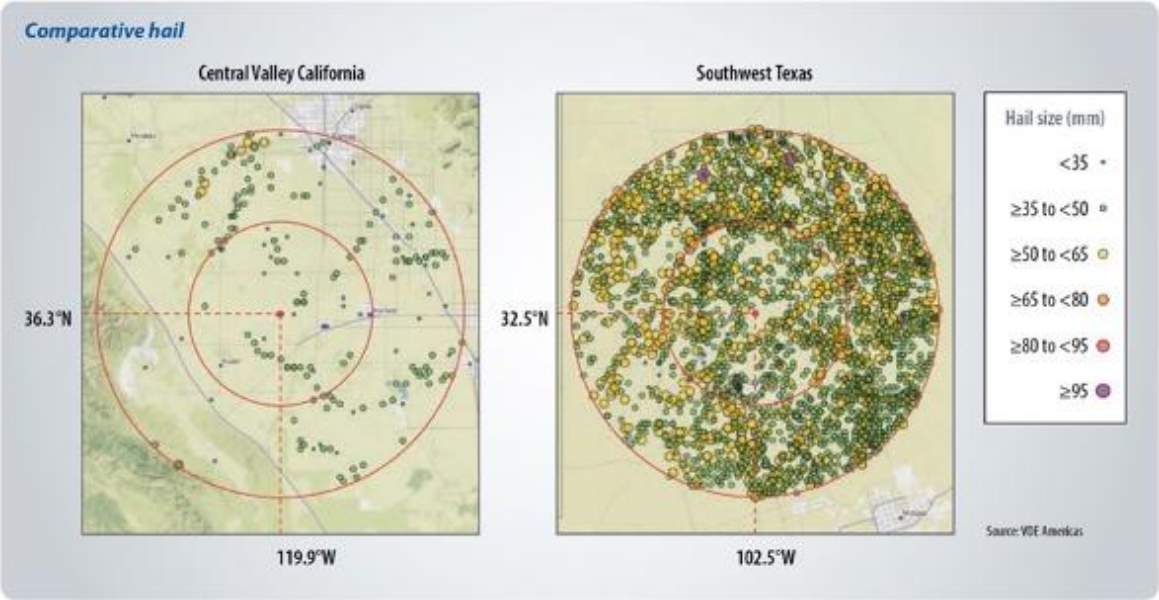

Figure 13: Comparative hailstone frequency and distribution for a low-risk location (California) versus a high-risk location (Texas) based on calibrated radar data [67].

4 SNOWSTORMS AND BLIZZARDS

4.1 Overview

Snow is practically ubiquitous across the northern hemisphere, occurring almost everywhere, at some altitude and at some point in time, as depicted in Figure 14. In a typical winter, snow covers at least 50% of the total land area and is the dominant form of precipitation; snowstorms are also generally predictable, i.e., snow occurs repeatedly in those regions for one or more winter months. Although the US National Weather Service (NWS) has no formal definition for snowstorms, the agency defines a blizzard as a snowstorm that 1) persists for a period of three hours or longer; 2) has sustained winds or frequent gusts in excess of 56 km/hr; and 3) creates low visibility conditions of less than 0.4 km.

While design parameters for snowy climates are described in the IEA Subtask 3.2 Report "Guidelines for the optimization of PV system key performance indicators" [78], the focus of this chapter is on extreme snowstorms and heavy seasonal snowfall. Although the objective in both cases is to shed snow as quickly as possible from the PV panels to minimize shading and lost generation, the challenge of shedding snow intensifies during record-breaking snowfalls, which are defined both in terms of accumulated centimetres of snow and the amount of land area impacted.

According to climate-change models, northern latitudes are likely to experience heavier than normal snowfall over shortened winter seasons, with consequences for PV arrays that are twofold: 1) extreme snow events can threaten the structural integrity of modules and mounting systems and 2) they can block irradiance from reaching the solar cells for extended periods.

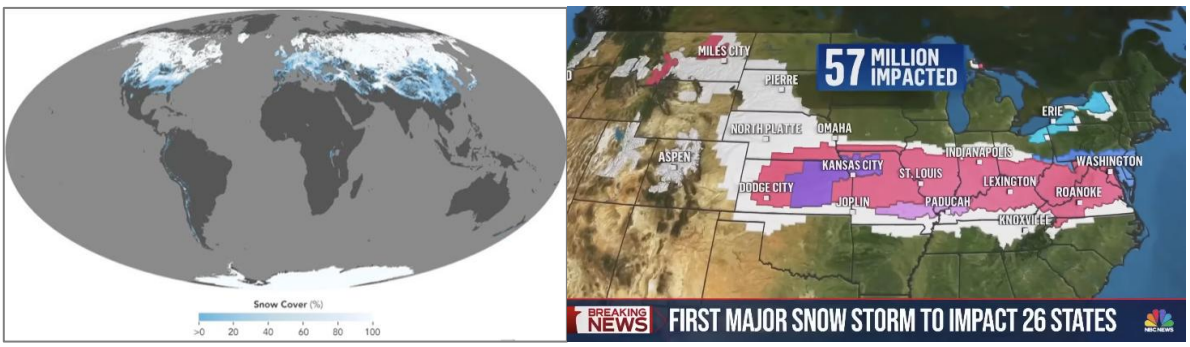

Figure 14: Global distribution of snow in January 2025 (left) showcases the large amount of land in the northern hemisphere typically covered in snow in winter. [Source: https://scence.nasa.gov/earth/earth-observatory/global-maps/snow-cover/]
In the US (right) single storms often sweep from the west to the east, potentially shading GWs of PV.

4.2 Operational impacts

4.2.1 Resource availability

As PV deployment expands at higher latitudes, resource availability in regions where solar and snow intersect is an emerging challenge. Throughout the winter months, snowstorms occur frequently, depositing large quantities of snow across the northern US, Canada, Europe and Asia. A snowstorm may sweep across thousands of kilometres, especially in the US, where many storms originate in the Rockies and move eastward. These massive storms can impact hundreds of gigawatts of PV, shading the panels with snow that might vary from a dusting to a deluge 100 cm or more deep. In addition, one storm can follow another, adding more snow to what is already present. When the snow reaches a certain depth, which varies based on temperature, humidity, windspeed and age of snow, energy generation ceases, and the PV plant effectively goes offline. Multiple research institutions around the world are therefore focused on 1) developing cost-effective and reliable strategies for accelerating snow shedding from modules; and 2) predicting and mitigating the loss of solar-generated power for storm-affected regions. Snow-removal strategies are discussed in section 4.3 below, as are models for quantifying energy losses attributable to snow. Accurate forecasting models, however, that would enable grid operators to manage both the generation loss and sudden ramp-rate of PV plants following a snowstorm, are still being developed. Regardless, identifying the underlying parameters for snow shading, and its corollary, snow shedding, is critical to the continued growth and grid penetration of solar in northern regions.

4.2.2 Power loss

Although the colder temperatures and high albedo of snow boost the efficiency of PV systems in in regions that consistently see snow in winter, the power losses attributable to snow-shading of PV systems are significant and impacted by multiple design parameters, including tilt angle, module architecture, module orientation, surface roughness and height above ground. To give an example, a 30-degree fixed-tilt utility-scale installation in the US experienced 90% power losses in the months of January and February under persistent snow conditions. Identifying and validating strategies that accelerate snow shedding and increase the availability of PV plants in winter is an important area of investigation as solar increases its generation footprint.

Ignoring snow cover as a factor in 30-year performance warranties can lead to overestimating power output. Including energy losses attributable to snow shading is therefore important for accurate long-term performance modelling to ensure proper financial assessment and system sizing. As the following sections illustrate, snow losses can be estimated using multiple existing methods, but none fully captures the variables involved, including module orientation, form factor, electrical architecture and non-uniform shedding patterns.

Measured losses from snow can be estimated if periods of snow cover are clearly identified, along with performance data, and if snow effects can be separated from other loss mechanisms, such as inverter downtime or low irradiance. Moreover, irradiance data only enable one to calculate the losses in real-time, rather than predictively. In addition, quantifying the economic impact of a single storm depends on the amount of time the array was covered, which in turn is determined by multiple variables, including snow depth, ambient temperature, wind speed, humidity, etc., and the cost of electricity.

4.2.3 Physical damages

In addition to reduced energy output, heavy snow can physically damage solar installations: modules can deflect under the weight, resulting in glass and cell cracking; ice dams formed from partially melted snow can shear the bottom frame from the module; and racks that are not properly engineered can collapse under heavy snow loads. Fresh snow and ice have densities ranging from 30–50 kg/m^3 and 800–900 kg/m^3 respectively but as snow ages and as temperatures rise, snow compacts and crystals will lose their dendrites, resulting in decreased porosity and greater weight per vertical millimetre. The weight of snow is also a function of ambient temperature and humidity. Moreover, the load on modules can increase over time if new snow arrives before the older snow is shed. Moreover, as snow sheds, its distribution and associated load stresses are non-uniform across the module surface and often concentrated along the lower edge of the module, putting the module in tension and stressing the frame. Yet another issue is that the shedding of large amounts of snow creates snow mounds under the array, high enough to block the lower portion of the module.

In cases of extreme snowstorms, depositing half a meter or more of snow on top of existing snow cover may bury the lower portion of an array. Snow obstruction is especially problematic for single-axis tracker systems, as shown in Figure 15. Unable to move through the deep snow, the tracker will experience both generation losses and motor stress.

Modules are rated for static mechanical loads according to IEC 61215-2, where simulated snow load is applied pneumatically, or by weights in a uniform and gradual fashion to the glass front and back surfaces excluding the module frame or cross support. The test is performed at room temperature, and a constant load of 5400 pascals is maintained for one hour on each side. These steps are repeated for a total of three cycles while monitoring the electrical continuity of the internal circuit [79]. The test may need to be repeated for different mounting configurations and safety factors. Modules can also be subjected to non-uniform loading conditions per IEC 62938, which calls for step-distributed non-uniform loading of a module at a specified tilt angle. Like the static load test, the non-uniform load test is conducted at room temperature. Field conditions, however, are strikingly different, as snow is repetitive, often accumulative, and always accompanied by cold temperatures as well as temperature swings.

Figure 15: Heavy snow load on a tracker system at the Michigan Regional Test Center (RTC), combined with high snow depth and some drifting, have rendered this system temporarily inoperable. Photo credit: *Paul W. Dice.*

In a recent study by Tanahashi et al. [80], heavy snow loads were examined using three PV test arrays in Shinjo, Japan. The test arrays were equipped with load cells built into the

mounting fixture at module tilt angles of 10°, 20°, and 30°. Snow pressure was largest for the 10° tilt array, with frontal loads along the leading edge of the row reaching up to 6–8 kN/m. Snow loading was progressively less for the 20°, and 30° tilt angles. As shown in Figure 16b and 16c, loads increased when the snow cover on the modules was contiguously connected to the snow on the ground.

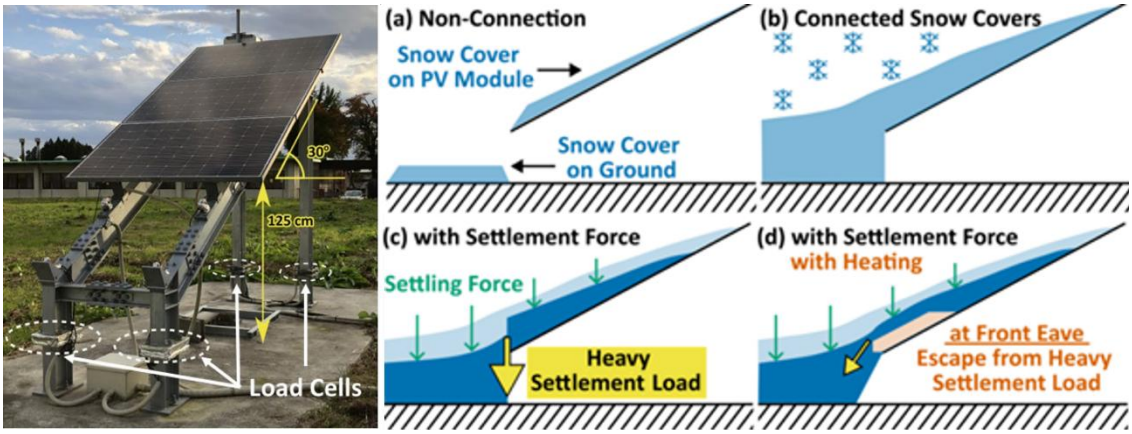

Figure 16: Experimental PV setup showing one of three subarrays with load cells. Depictions in a), b), c), and d) show the process of snow accumulation, the formation of a contiguous snow pile, settling and loading of the module, and melting by backside heating [80].

Under the right meteorological conditions, wind can be a powerful force in removing snow from modules, but wind also plays a role in snow accumulation, especially in Arctic regions, where the snow has a low-moisture content. Wind can form snow drifts, especially in the wake of obstacles such as ridges, buildings, or PV arrays, which can concentrate snow in specific areas, such as between rows. A case study from Svalbard, Norway, showed that snow drifting partially covered a ground mounted test array consisting of four mock-up module rows, each 10 meters wide [81]. A subsequent simulation study showed that raising the modules decreased drifting, but increased racking costs. One can also opt for a lower tilt angle, effectively raising the modules, or change the azimuth to put the modules parallel to prevailing winds but both options result in lower energy yields [82].

Snowdrifts can also be problematic for rooftop PV systems [83]. Figure 17a shows a photogrammetry model of the depth of a snowdrift on an industrial rooftop-mounted PV system in northern Sweden [84]. An adjacent wall blocked wind-blown snow, causing a snowdrift to form on some modules, deep and heavy enough to destroy the modules, as seen in Figure 17b. Note that these modules were clamped at the corners, contrary to manufacturers' recommendations, highlighting the fact that proper installation may have prevented the modules from collapsing.

a). 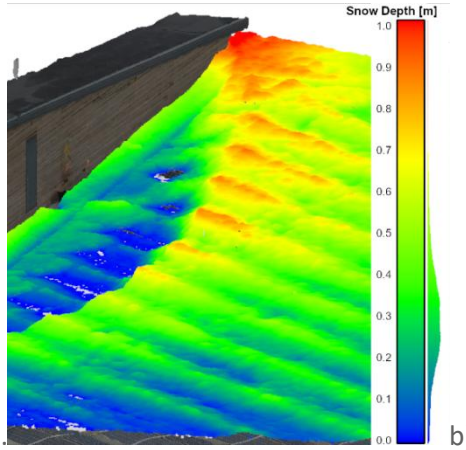

b). 

Figure 17: a) 3D-model reveals weight distribution of snow on an industrial rooftop PV system; b) visible image of incorrectly mounted PV modules damaged by the snowdrift. Photo Credit: *Research Institute of Sweden*.

In addition, the rapid adoption of 182 mm (M10) and 210 mm (G12) cells, which constitute approximately 31% and 62% of the market in 2025, respectively [85], has introduced reliability concerns. The newer large-format modules now have dimensions up to 2.3 m x 1.3 m (30 kg), but are not typically reinforced for heavy snow loads [86]. Burnham et al. [87] are conducting a comparative analysis of multiple module technologies (different cell sizes, form factors, front and back sheets, etc.) and mounting architectures (fixed-tilt vs tracker) to evaluate their robustness in winter (see Figure 18). Of specific interest are the multiple climatic stressors not captured by certification testing: namely the accumulative, repetitive, additive wind and snow loads, and related low temperatures, which increase cell susceptibility to cracking. The results of this work, which will be published in 2026, is intended to i inform the design of winter-robust systems.

Snow loading also suggests the possibility of cell cracking, which can have a variety of causes related to physical stressors. Studies suggest that cells become more brittle as the ambient air temperature drops, meaning that crack formation is more likely in cold and snowy environments. Interestingly, preliminary data suggests that power loss caused by cell cracks (excluding hailstorm cell damage) is around 3% higher in snowy versus moderate climates and up to 6% higher in snowy versus humid/dry climates [88]. There are also indications that glass/backsheet modules are more susceptible to load-induced crack formation when exposed to cold temperatures and that some modules rated for 3.6 kPa or higher can sustain damage at loads as low as 1.0 kPa [84], [89], [90]. At the time of writing, field testing for different module designs and snow loads is underway to better model and predict cell cracking and enable more robust module choices for cold and snowy regions. Studies are also underway to compare cell interconnects, such as multi-wire ribbon technologies, which are associated with less cell cracking [91].

Figure 18: Test array at the Michigan RTC for Emerging Solar Technologies in Calumet, Michigan, USA. A comparative reliability analysis is underway of six distinct module technologies, varying in dimensions, cell size, front glass and back sheet, with each module monitored for snow loading, wind loading, deflection, temperature and DC power. At the end of each winter, all modules are evaluated for cell cracking using electroluminescent imaging. Photo Credit: *L. Burnham*.

In addition to PV test sites, data on module durability may be supplemented with field data from PV arrays experiencing heavy snow loading. Japan's National Institute of Technology and Evaluation (NITE) noted damage due to heavy snow and ice for 43 PV systems in the Tohoku and Hokkaido regions in 2018-2021. The PV arrays in this study were a mix of medium (50 kW–2 MW) and large (> 2 MW) systems. The combined capacity of affected systems was approximately 30 MW, with the most common damage being deformation of the module frames [92]. In a second NITE study [93], a small category (10–50 kW) was added to the medium and large-scale array reporting results for snow. The second study occurred from April 2021 to March 2023 and covered 65 arrays mostly located in the Hokkaido, Tohoku, Chubu, and Chugoku regions. Noting a variety of mild to severe damage events correlated to periods of heavy snowfall, NITE recommended the use of surveillance cameras to detect snow quickly, and regular site visits to remove accumulated snow.

4.3 Mitigation strategies

Mitigation strategies, which are largely focused on utility-scale installations and must tackle the dual challenges of reliability and availability, fall into three categories: active shedding, passive shedding, and design optimization. Active methods involve mechanical or thermal interventions; passive methods include the application of coatings that alter the topology of the cover glass to create hydrophobic or hydrophilic surfaces; design methods include the use of bifacial/frameless modules, higher tilt angles for fixed-tilt systems, and adequate ground clearance for both fixed-tilt and tracker arrays.

4.3.1 Active shedding methods

Active methods include internal heating of the module, external heating on the front or back, mechanical removal with a rake or blower, and increasing the tilt angle of a single-axis tracking

systems. In recent years, interest has grown in generating heat to melt snow by injecting a controlled forward-current bias into modules [94]. Aarseth et al. in Oslo, Norway, for example, used commercial DC power electronics to apply a current of 10 A (forward bias of 45 V) to each module of a 1 MW rooftop array, concluding that bias heating is effective for snow shedding, but energy and economic payback times depend on weather conditions and electricity rates [95]. The amount of energy needed depends on the ambient temperature, wind speed and snow volume and also the system design, with less energy needed for high tilt angles, where snow slides more readily than for lower tilt angles. The long-term economic and reliability benefits of current injection, however, remain unknown and untested on an industrial scale. The impact of forward bias heating on module degradation or bypass-diode reliability, for example, has not been investigated. Nor is it clear how the strategy might impact module warranties. Another challenge is that melted water must be transported away from the system to avoid refreezing on the array or rooftop, especially for commercial rooftops with parapets.

A second method involves a resistive element, such as a transparent conducting oxide or patterned conductor that is applied to either module surface. In a study by Tanahashi et al. [80], a copper mesh was applied to the backsheet; results show that melting created an air gap and discontinuity between the snow on the module and snow on the ground. As shown in Figure 16d, the gap reduced the total load on the modules. Accumulated snow on the ground exerted a downward force on the PV array when snow on the module and ground was contiguous [80]. Li et al. combined both active and passive methods by applying resistive heating, combined with transparent hydrophobic aluminum nanostructures, to the front side to enhance snow sliding [96]. The practicality, including cost and reliability considerations, of this approach, has not been demonstrated, however.

A third active-shedding method is manual cleaning but the latter can cause module damage if snow rakes [97] and other equipment strike the modules. The method is also labour-intensive and most effective as an initiator of shedding on high-irradiance days. A fourth approach is to develop advanced stow strategies for single-axis tracker systems. Under the right meteorological conditions (such as low temperature and low irradiance (see Figure 15)), snow can adhere to PV modules, even at a 52° tilt. Advanced tracker control algorithms can dictate stow strategy based on anticipated snow, ambient air temperature and prevailing wind direction. The key is timing: too little snow and generation is lost; too much snow and severe strain is put on the motors. Research underway at Michigan Technological University suggests a high tilt-angle, combined with stowing modules away from the wind direction, is a promising strategy [98].

4.3.2 Surface coatings

Deployment of snowphobic and icephobic coatings by the airline and shipping industries is a widespread and common practice, but coatings specifically formulated for solar panels face two challenges: 1) transmissivity must be maintained over time, with minimal UV-induced degradation of the coating; and 2) the coating must be resistant to delamination and surface abrasion over the life of the PV panel. The best-known study of snowphobic coatings so far focused on transparent polymeric-based coatings, which reduce the detachment force of ice, enabling passive snow shedding even at sub-zero temperatures [99]. Field trials of this new coating in Alaska have demonstrated higher output for coated modules compared to uncoated reference modules [100], [101], but durability data is lacking. Demonstrations of next-generation technologies are planned in northern Michigan to validate their performance and potential for PV applications.

4.3.3 Passive shedding methods, module selection and design considerations

Compared to framed monofacial modules, bifacial and frameless module architectures have inherent snow-shedding advantages. Frameless module designs, although impractical for large-format crystalline silicon modules, will shed snow as much as 50% faster than framed counterparts [102]. While bifacial modules shed snow at a lesser rate than frameless modules, they are still are distinctly advantageous in snowy climates because they produce more energy under high albedo conditions, as is typical in winter; they also generate power when the front surface is snow-shaded [103], [104]. For example, Hayibo et al. documented a bifacial gain of 19% for a bifacial 420 kW system compared with a nearby 1.2 MW monofacial system in Escanaba, Michigan [105]. Burnham et al. compared monofacial modules to framed and frameless bifacial modules co-located on dual-axis trackers [106]. The bifacial modules shed snow better than the monofacial ones due to backside irradiance, which increased the module temperature. Compared to framed modules, frameless bifacial modules had an even greater potential to shed snow.

In addition to the choice of module, the design of fixed-tilt racking also affects how an array performs in snowy conditions. Snow sliding generally occurs best at tilt angles of at least 45° [107]. For sites experiencing heavy snowfall, steeper angles may be recommended. Steeper-than-latitude tilt angles may reduce annual energy production, but can result in better snow shedding, protect modules from damaging snow loads, and improve the collection of front and backside albedo (Figure 19).

One negative consequence of accelerated snow shedding, however, is the possibility that the shedding of large amounts of snow before significant melting or natural removal via wind or sublimation may result in mounds that accrue at the system's lower edge, blocking further snow shedding and causing physical damage to the modules (see Figure 15).

Figure 19: Example of a hybrid orientation system installed by Sandia National Laboratories at the Michigan RTC. Analysis is underway of the relative performance of the south-facing fixed-tilt vs vertical east- and west-facing bifacial modules, which collect almost no snow. Photo credit: *Paul Dice.*

Snow shedding and subsequent formation of mounds also depends on racking configuration. Elevating the racking above the ground to account for average snow depths in winter at that location should, in most cases, provide adequate space for snow to shed and pile [107]. The number of rows can also be limited to decrease the volume of snow that can form mounds.

4.4 Quantifying Snow Losses

Empirical Method

For this method, which is based on historical data, snow losses are quantified by comparing the energy generated in winter with the amount of energy that would be generated under snow-free conditions. A heated plane-of-array (POA) pyranometer can provide irradiance data needed to compare measured versus modeled snow losses. The challenge is finding a way to identify exactly when the array is covered by snow and by how much. Other challenges include monitoring the depth and density of snow on the panels themselves, which in turn reflects ambient meteorological conditions, the transmissivity of the snow, the uniformity or non-uniformity of snow distribution on each panel and the panels' electrical architecture. Overall, the objective is to quantify snow losses by determining exactly when and how much of, the array is covered in snow and comparing the measured energy produced during these periods to the simulated snow-free output.

For research sites, time-series POA digital images, combined with image-processing algorithms (see Figure 20), can quantify the percentage of snow cover at the module- and string-level [108], [105]. Although this method is historic rather than predictive, it enables one to compare the performance of different system designs. Forecasting energy production for grid management is a more complex endeavor, requiring snow-loss algorithms.

Modeled Method

Most snow-loss models predict snow shedding based on ambient temperature/irradiance, and tilt angle. Several modelling methods use empirically derived factors based on data collected from test arrays, although these results do not represent all module technologies, mounting configurations, locations, or climates. Pawluk et al. [109], identified 11 snow-loss models. Some were validated at multiple sites [110], [111], [112], while others remain relatively untested. Of these, the Marion et al. [111], [113], [114], Townsend and Powers [110], SunPower [115], and Andrews et al. [116] models are the best documented. The comparison and validation of different snow-loss models using data from utility-scale arrays would significantly help integrate snow-loss modelling into best-practice procedures [117].

Figure 20: Snow accumulation on PV modules with a single-axis tracker. The yellow quadrilaterals indicate the segmentation of the modules for analysis of non-uniform shedding patterns. Photo Credit: *Laurie Burnham*.

4.5 Key Takeaways and Recommendations

Under extreme snow conditions, where a single storm may deposit up to a meter of snow, the objectives are to 1) shed snow as quickly as possible from the panels in order to restore generation; 2) reduce load damages by designing systems, including the hardware as well as modules, that can withstand the heavy weight of snow; and 3) raise the height of the mounting system to minimize the impact of snow mounds on the modules.

Recommendations for ***accelerating snow shedding*** include the following:

- Implement advanced stow strategies for single-axis tracker systems that minimize snow adhesion based on tilt angle and wind direction.
- Ensure that the lower edge of each row is high enough to allow snow to freely shed and accumulate, considering the maximum expected snowfall in the region.
- Install bifacial modules, which absorb rear side irradiance, and can therefore shed snow faster than monofacial modules.
- If practical, given other design, installation, and procurement constraints, consider frameless modules instead of framed modules.
- Consider installing an auxiliary array of vertical bifacial modules for backup generation to meet critical load.
- Select modules that are more robust (thicker front glass, smaller surface area)
- Install racking/tracking systems that are well-engineered with posts, rails, purlins and bolts that can withstand repetitive and dynamic wind loading.
- Conduct visual inspections post-winter to look for any damages and thermally image a subset for evidence of hot spots.

5 DUST AND SANDSTORMS

5.1 Definition and frequency

Dust and sandstorms (DSSs) are characterized by large amounts of particles suspended in the atmosphere, reducing the intensity of irradiance reaching the Earth's surface. These events typically originate when strong winds, generated by thunderstorms or strong air pressure-gradients, blow across arid and semiarid regions [118], [119]. They can have substantial local, national, and international consequences in terms of PV energy production.

Figure 21 shows the spatial distribution of clear-sky radiation, dust optical depth (which expresses the dust-induced attenuation of light as it is transmitted through the atmosphere; see Subchapter 5.3.1 for details), and cloud cover [120]. As observed, the impact of suspended dust, expressed by the dust optical depth, is a significant problem for PV systems because the geographic regions with high solar potential (i.e., high clear-sky radiation and low total cloud cover) are also those that are more likely to experience DSSs. Dust storms mainly affect arid and semi-arid regions, but the dust they generate can also travel long distances, reaching Europe and other continents from their origins, say, in the Middle East [121], [122]. Given the widening global distribution of PV systems and the extensive area affected, dust storms have the potential to cause significant macro-scale effects: the sudden drop in PV power plant generation attributable to a DSS has the potential to temporarily destabilize national electricity grids [120].

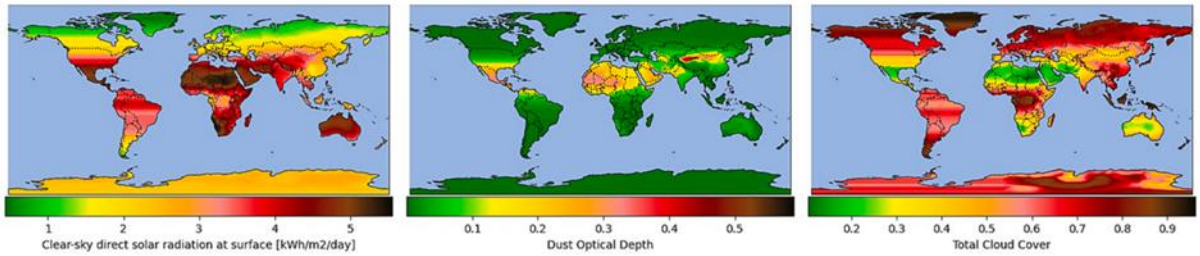

Figure 21: Maps of average clear-sky direct solar radiation (left), dust optical depth (middle), and total cloud cover (right) [120]. Data is represented as annual averages.

5.2 Associated risks

Dust and sandstorms can impact PV systems in two ways. First, there is the concurrent effect of reduced intensity of surface irradiance, attributable to the absorption, reflection and scattering of sunlight by the suspended particles. Specifically, the drop in Global Horizontal Irradiance (GHI) and Direct Normal Irradiance (DNI) can be as high as 40-50% and 80-90%, respectively [123]. And a second, potentially longer lasting effect of DSSs, is the increased accumulation of particles on the PV module surface (i.e., soiling). Soiling reduces the module's energy yield, and its effect can last after the sky has cleared, with reported persistent losses as high as 7% and 20%, for example, after DSS events in Portugal and in Saudi Arabia [121], [124].

The following sections present two case studies from locations with different climates, namely Qatar and the Iberian Peninsula. These locations are of interest because they show the impact of dust storms on sites with different soiling patterns: Qatar is exposed to higher and more consistent soiling throughout the year, while countries such as Spain and Portugal experience seasonal soiling, with most of the losses occurring in summer.

5.2.1 Qatar/Arabian Peninsula

The Middle East and North Africa (MENA) region, including the State of Qatar, has high levels of irradiance throughout the year and on that basis is economically attractive for large-scale PV. However, frequent DSSs are major challenges for PV in this area.

After an extreme DSS event, in April 2015, the energy yield of a system in Doha, Qatar, dropped by more than 50% (see Figure 22). Even if that event is considered the most severe episode in decades, DSSs of lower but still substantial severity are not uncommon. Javed et al. [125] estimated that DSSs occurred on 10% of the days between 2014 and 2019 in Doha, with consistently higher percentages in the summer months (June to September). The seven most severe DSSs resulted in PV performance losses per event that exceeded 5%, whereas 55 less-intense DSS events still led to losses higher than 2%.

The authors also reported that, on DSS days, the average daily airborne particulate matter with a diameter 10um and smaller (PM_{10}) ranged from 115 to 339 µg/m^3, against an average of 89 µg/m^3 on clear days [125]. They measured an attenuation in solar radiation due to the suspended particles during DSSs of 8%. Additionally, they found that soiling losses increased at higher rates during DSS days (1.23%/day), compared to clear days (0.42%/day), leading to average soiling rates of 0.52%/day in Qatar. Although, soiling losses dropped immediately after the DSS event due to the removal effect of wind, Javed et al. [125] nonetheless concluded that DSSs increase soiling losses in Qatar by a factor greater than 20%.

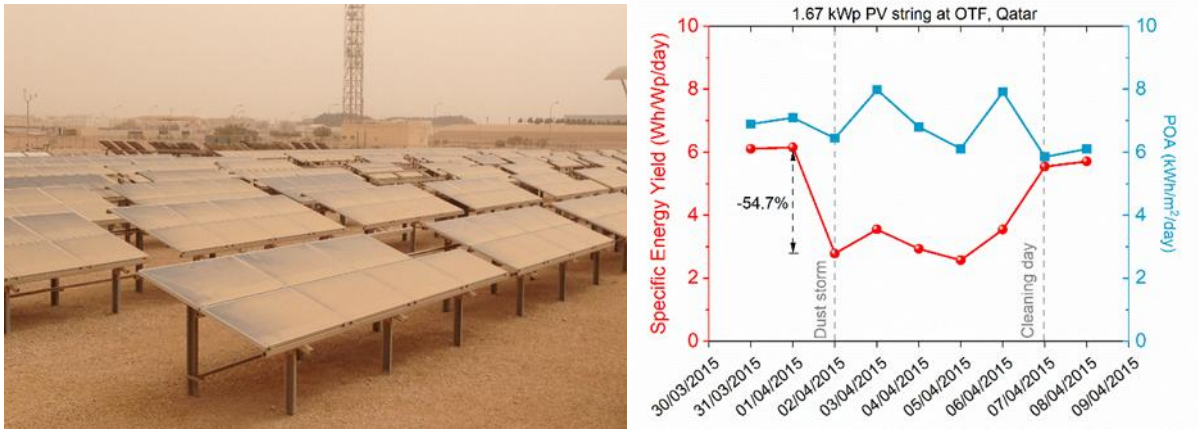

Figure 22: Dust storm in Doha, Qatar (02/04/2015) at the Qatar Environment and Energy Research Institute's Outdoor Test Facility. Dust-covered panels are depicted in the photo (*left*); The drop in energy yield (red) relative to available irradiance (blue) is shown (*right*), with a power drop of more than 50% in one day relative to available irradiance. Output is restored as the result of cleaning.

5.2.2 Iberian Peninsula/Europe

Because of prevailing wind patterns and its proximity to the Sahara, the Iberian Peninsula is often exposed to dust intrusions, with more severe consequences than other regions of Europe. An extreme dust storm event occurred in the second half of March 2022, affecting most of the peninsula for 17 days [120]. The high concentration of suspended dust and sand particles and the concurrent adverse weather conditions lowered Spain's PV energy output by 50% over a period of two weeks. On the worst day, the national PV capacity missed its expected production by more than 80%. However, because of the extraordinary amount of rainfall, which provides "natural" soiling removal, in that period no substantial increase in soiling loss persisted.

In contrast, two dust intrusions registered in Portugal in February and March 2017 were followed by significant decreases in energy production due to soiling (see Figure 23). Specifically, record-breaking power losses as high as 8% were measured during the first event in the outskirts of the city of Évora, Portugal [121]. The second event was less significant, with losses only as high as 3%. This limited impact was mainly attributed to the lower dust concentration and to the shorter duration of the second dust storm.

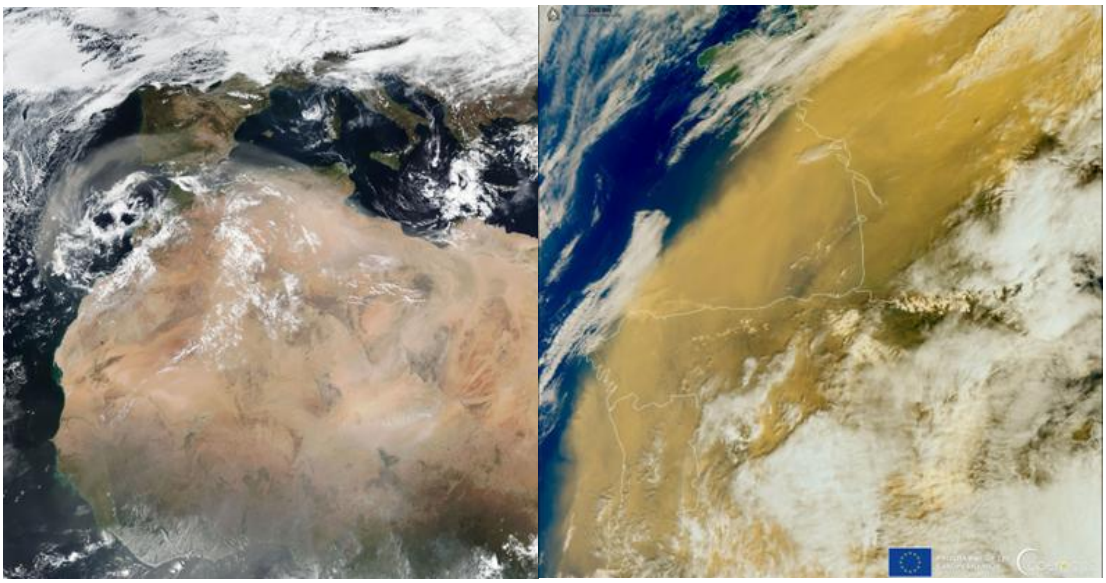

Figure 23: True-color images *(left)* taken by the Visible Infrared Imaging Radiometer Suite (VIIRS) instrument aboard the NOAA/NASA Suomi NPP satellite (21 February 2017); and image *(right)* from the European Union, Copernicus Sentinel-3 satellite of 15 March 2022, showing the Saharan dust cloud engulfing the skies over France, Spain and Portugal [126].

5.3 Recommendations

5.3.1 Monitoring

Both real-time monitoring and short-term forecasting are essential to limiting the negative effects of DSSs on PV. The occurrence of extreme dust storm events can be tracked and predicted based on aerosol optical depth (AOD) and dust optical depth (DOD), dimensionless parameters measuring the extinction of solar radiation in the atmosphere. Higher values of either AOD or DOD indicate reduced visibility and less solar radiation reaching the Earth's surface. Whereas AOD measures the columnar aerosol load (i.e., the combined contribution of dust, smoke and other particulates to the attenuation of solar radiation), DOD only accounts for suspended mineral dust particles in the atmosphere. DOD is therefore preferred for DSS monitoring because it excludes the non-dust aerosols that are not directly linked to dust storms. However, AOD is more commonly adopted in practice due to the wider availability. AOD and DOD values can be either ground-measured or derived from satellite or reanalysis data (see Table 4, or [127] for a more comprehensive and detailed list).

Table 4: Examples of aerosol data sources.

Source	Description	Reference
AERONET (Aerosol Robotic Network) program	Ground-measured aerosol properties in several locations worldwide	[128]
ModIs Dust Aerosol (MIDAS)	Gridded DOD values from the interpolation of satellite and reanalysis data.	[129]
ECMWF Atmospheric Composition Reanalysis 4 (EAC4).	Global reanalysis of atmospheric composition.	[130]

Gkikas et al. [131] classified DSS on day *d* as "extreme" if:

$$AOD(d) > \overline{AOD} + 4 \cdot \sigma_{AOD} \quad (1)$$

where $\overline{AOD}$ and σ_{AOD} are, respectively, the average dust optical depth in a location and its standard deviation. Similarly, DSSs have been classified as "intense" if:

$$\overline{AOD} + 4 \cdot \sigma_{AOD} > AOD(d) > \overline{AOD} + 2 \cdot \sigma_{AOD} \quad (2)$$

Dust, however, only partially contributes to the optical effects of the aerosol load. For this reason, Papachristopoulou et al. [126] suggested replacing AOD in previous equations (1, 2) with DOD. Additionally, in February 2024, Copernicus launched an Aerosol Alerts service that informs users on the occurrence of DSS events depending on the geographical areas and aerosol species of interest [132].

Particulate matter indices, such as PM_{10} and $PM_{2.5}$, can also detect the occurrence and the magnitude of dust storm events, and are available both in ground-based or satellite-derived datasets. Specifically, PM_{10} thresholds of 100, 150 and 200 µg/m^3 have been employed to detect the occurrence of DSS in various studies [133], [134], [135], [136]. Alternatively, DSSs have been identified in conditions of average PM_{10} above 200 µg/m^3 for more than 4 hours in a day and a maximum hourly value above 250 µg/m^3 [137]. However, it should be noted that PM_{10} and $PM_{2.5}$ offer only a partial overview of the aerosol load, as they are mostly related to the lower part of the atmospheric column only [138].

As mentioned above, DSSs can increase soiling accumulation rates, leading to prolonged performance losses even after the sky has cleared. As already described in a previous IEA PVPS Task 13 report [139], soiling can be estimated through models or measured using sensors. Soiling stations are the most common soiling measurement solutions: they compare the electrical outputs (either the short-circuit current or the maximum power output) of two PV devices, one cleaned and one left to soil [140]. However, it should be highlighted that the dust storm-induced accumulation of soiling can be significantly non-homogenous. This means that measurements based on the short-circuit current and the maximum power output can return different estimates [141]. For example, when investigating the February 2017 event in Portugal (see above), Conceição et al. [121] found an 8% decrease in power output (see Figure 24) but the loss in short-circuit current was limited to 3% because of bypass-diode activation. For this reason, maximum power output measurements are preferred.

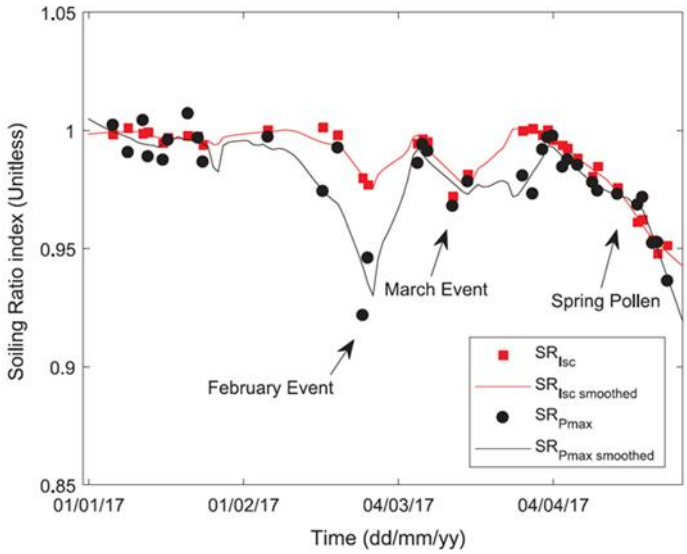

Figure 24: Soiling ratio index (ratio of the actual electrical output to the expected electrical output under conditions of no soiling) for a rural region near Évora city, Portugal, from January to April 2017 [121]. Measurements compare short-circuit current (Isc, black) to maximum power (Pmax, red).

5.3.2 Mitigation

Mitigating the effects of dust storms means reducing soiling-induced losses. In soiling-prone locations, such as Qatar, the cumulative impact of regular soiling typically causes more losses than the occurrence of acute dust storms. In contrast, in locations such as southern Europe, soiling losses are substantially higher when dust storms occur. Under both scenarios, mitigation protocols can be developed and deployed on a regular basis.

For regular soiling, mitigation can be either preventive or corrective [139]. Prevention aims at reducing soiling, by lowering its deposition rate or by facilitating its natural removal. Wherever possible, in the presence of a DSS, modules should be positioned upside down, or at least at the highest possible tilt angles away from the wind to reduce front-surface soiling. Note that, despite promising results [142], trackers are still limited by the maximum angle (typically ±45° to ±60°) to which they are designed to move. Also, high wind conditions, which are typical of many DSS events, can put the PV system at structural risk, rendering the high-stow option unfeasible. Another alternative is to use "dust walls", which aim to modify wind patterns so most soiling particles are deposited away from the PV system [143], but the technology needs to reach a more mature state before being widely deployed. Anti-soiling coating technologies are yet another strategy to minimize dust adherence to the front surface of PV panels, reducing soiling accumulation rates and, therefore, the need for cleaning [144].

Corrective actions include removing soil from the surface of modules once it has already accumulated. This strategy can be executed via manual, semi-automatic, and fully automatic cleaning methods [144]. However, soiling caused by dust storms has been found to be more difficult to remove than “regular” soiling because of the density of soil on the module. As the soiling density increases, the cleaning efficiency drops, potentially making regular cleaning technologies (such as automated robots) ineffective. This means that, after DSS events, multiple cleaning runs might be needed to remove the accumulated particles. Also note that active cleaning methods may degrade the modules’ anti-reflective coatings, resulting in a small drop in efficiency, although the immediate gains will be substantial.

6 HEAT WAVES

6.1 Definition

There is no universal definition of heat waves. Some climate studies base the definition on a temperature threshold or a percentile of temperature and minimum duration, such as a period of three or more consecutive hot days and nights. In the calculation for the years 1969−1998, a hot day (night) is when the daily temperature exceeds the long-term daily 95th percentile for the summer season (June-September in the Northern Hemisphere; December-March in the Southern Hemisphere). Another definition states that a heat wave must span at least six consecutive days with maximum temperatures exceeding the local 90th percentile for the historical period 1961−1990. Yet another definition--put forth by the STARDEX (STAtistical and Regional dynamical Downscaling of EXtremes for European regions) project—defines a heat wave as a sequence of at least six consecutive days with daily maximum temperatures of at least 5°C above the climatology. The climatology is calculated for a 5-day window centered on each calendar day in the reference simulation [145].

6.1.1 Projected changes

Several IPCC reports predict more intense, longer-lasting heat waves, including pronounced heat waves over western Europe, the Mediterranean, and the southeast and western United States, the result of circulation changes attributable to the increase in greenhouse gases. But these scenarios or models show non-uniform changes (see Figure 25), meaning patterns do not scale well for extremes, making heat waves hard to predict [146].

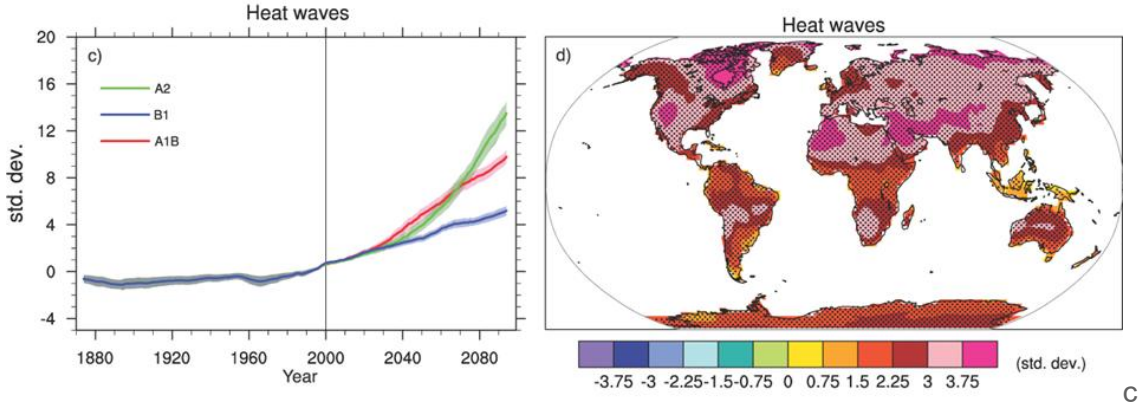

Figure 25: Left: globally averaged changes in heat waves (defined as the longest period during the year with at least five consecutive days when maximum temperatures are at least 5°C higher than then climatology of the same calendar day) according to different scenarios. Right: changes (deviation) in spatial patterns of simulated heat waves between two 20-year averages (2080-2099 minus 1980-1999) [147].

Projections for changes in the earth's temperature-at-surface (TAS)—according to the IPCC climate scenario Rapid Concentration Pathway (RCP) 8.5—varied from 3 to 5°C for the end of the century and have an associated mean induced change in the potential PV production (PVpot) in southern and eastern Europe of -3% (see Figure 26) [148].

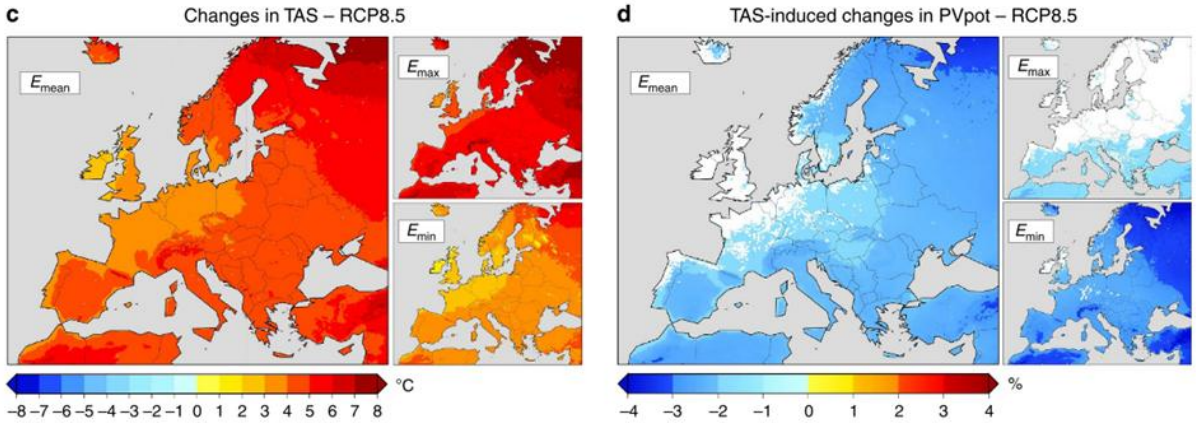

Figure 26: Left: Climate change projections represented by TAS (temperature at surface); Right: Projected increase in TAS is likely to impact PVpot by the end of the century (2070-2099 versus 1970-1999) [148].

6.2 Impact on PV production

PV generation is negatively impacted by temperature, with a linear decrease in cell performance when temperatures exceed 25°C. Research on crystalline silicon-based cells found that for every 1°C rise in temperature above 25°C, the cell's efficiency reduces by 0.2% to 0.5% in relative terms. Devices in a PV system such as the control system, cables and the inverters are also affected by high temperatures, resulting in lower energy output and lower capacity of underground conductors [149]. Cables are also vulnerable to thermal stress, and will expand and contract, exerting mechanical stress on the PV system's electrical inter-connections, which can be compromised, unless the system is designed appropriately.

Heat also contributes to inverter under-performance, with most inverters applying a temperature derating (i.e. limiting output power) when an ambient temperature threshold is passed, which is 40°C or 50°C. This temperature derating as %/°C varies by inverter make and model, with the voltage of the array, inverter MPPT operational window and grid connection voltage affecting the value in practice. A study of around 1,300 PV systems with a total of 23,000 inverters across Germany reveals an increase in overheating warnings for inverters, correlated with rising ambient temperatures, Although the actual failure rate was comparatively low, more data is needed from extreme environments to understand the impact on inverter efficiency [150].

6.2.1 Effects from natural disasters

Wildfires are a common consequence of heat waves, and there have been several cases where dry vegetation beneath ground-mounted solar panels has caught fire and spread across solar farms. Two such incidents occurred during the July 2022 heat wave in Europe (see Figure 27), where grass fires, likely triggered by an electrical arc fault from a connector or inverter, ignited and spread quickly through the dry vegetation at a 30 MW solar farm in the Netherlands and a 20 MW solar farm in the United Kingdom [151]. More information on wildfires can be found in the next chapter.

Figure 27: Grass fire under ground-mounted solar panels in the United Kingdom [151]. Source: Dailymail UK (https://www.independent.co.uk/climate-change/news/dorset-solar-farm-fire-verwood-b2121279.html**).**

6.3 Two types of heat waves

Heat waves can be either dry, having relative humidity below 33%; or moist, with relative humidity above 66%. Both types can occur in the same region, e.g., in East Asia, where dry heat waves prevail over the northwestern region, adjacent to the main desert regions, and moist heat waves typically occur in southern the southern region, closer to coastal areas [152].

An example of a dry heat wave comes from Fraunhofer ISE's monitoring station in Israel's Negev Desert (at 30.8° latitude). The site, Sde Boqer, experiences both high irradiance and temperature conditions, but has low humidity. The average annual irradiation is around 2,276 kWh/year/m², with an ambient temperature of 20.4°C, effective module temperatures of 35.4°C, wind speeds of 2.0 m/s, and relative humidity of 13% at 47°C. Record-breaking heat waves have occurred here approximately every two to four years, including 2010, 2012, 2016, 2018, 2020, and 2021.

A heat wave recorded from May 14-22, 2020, reached temperatures around 40-43°C, depending on the location. Although no absolute temperature records were broken, the heat wave was notable for its extended duration [153]. Figure 28 illustrates the daily average electrical parameters of a reference silicon PV module deployed in Negev since 2011. The dotted green lines indicate the change in average values before and during the heat wave, with Pmpp dropping by 12.5 W (9.8%), Isc by 0.3 A (5.7%), and Voc by 1.1 V (3.2%). When calculating the temperature coefficients (TC) for each of these parameters based on outdoor measurements for that year, the TC_{Pmpp} is -0.39%, TC_{Isc} is -0.0043%, and TC_{Voc} is -0.33%.

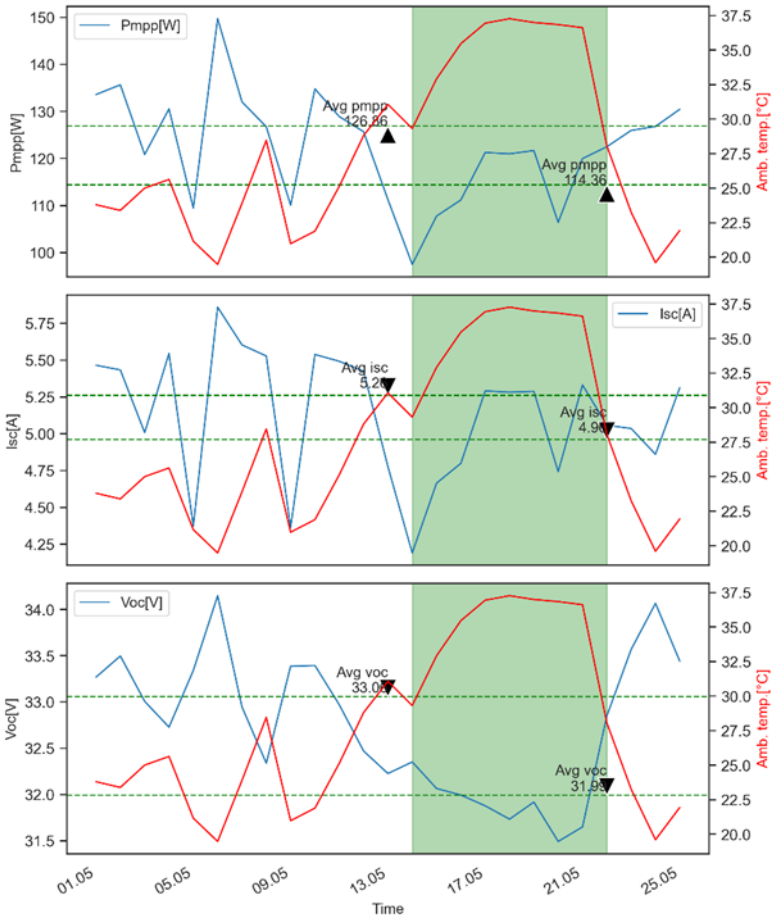

Figure 28: Changes in Pmpp, Isc and Voc for a PV module in Negev, Israel in May 2020. Ambient temperatures (red line) during a heat wave from May 14-22 (green area) are shown. Total average values before and during the heat wave (dashed green lines) show reduced module performance. Data is from Fraunhofer's Outdoor Performance Lab – Testsite Negev Desert.

6.4 Degradation effects of heat

Kaaya et al. present a model that considers climatic loads on PV modules in different world regions [154]. The results confirm that high temperature is a primary accelerator of degradation; a mapping of specific degradation mechanisms can be found in [155]. The researchers note that degradation rates can reach up to 0.8%/year in the hottest areas of Europe (southern Spain and Portugal), and globally up to 1.4%/year in regions near the equator. Degradation also manifests itself in component failures commonly found in desert climates, including encapsulant discoloration, back-sheet chalking and/or delamination. Interestingly, even though UV levels and temperatures are high in deserts, low humidity decreases the effect of photo-degradation. The annual degradation rate for an arid climate is estimated to be 0.74%/year, corresponding to 21.4 years of operation before reaching 80% of initial performance.

A study led by Theristis comparing degradation rates for modules deployed across different US climate zones found that the modules installed in the hot, humid subtropical climate of Florida degraded at almost twice the rate (median Rd value of −1.12%/year) of the same modules

installed in New Mexico (hot and dry) and Colorado (cool), which had Rd values of −0.56%/year and −0.61%/year, respectively [156].

6.5 Mitigation strategies and key takeaways

- **System planning:** Inverters should be installed in places that will minimize overheating, i.e., well-ventilated and shaded locations. At a minimum, they should not be installed near a heat sink, such as a concrete structure or building; should be separated from each other, and equipped with a shade cover, if existing shading is inadequate
- **Module selection:** PV modules that have low temperature coefficients, such as cadmium telluride, heterojunction, and TOPCon, are good options for high-heat locations.
- **Degradation rates:** More analysis of technology- and location-specific degradation rates is needed to increase the accuracy of performance models and LCOE calculations.
- **O&M practices:** Because heat waves are often associated with drought, which creates dusty conditions, modules should be cleaned following prolonged heat waves. In addition, they should be inspected and thermal-imaged to enable the early detection of spot shading, hot spots, or cell fractures.
- **Cooling technologies:** Some companies offer active cooling systems that spray recycled rainwater over the top of the panels during hot days, thereby lowering a module's operating temperature. Other solutions being researched include hydrogels attached to the PV module and the co-location of solar farms with wind turbines for cooling airflow [151] but none of these options have been broadly adopted.

7 FLOODS

7.1 Overview

Climate change has caused an increase in the frequency as well as severity of flooding across much of the world. The severity of flooding has broken historical records in many areas, including areas with arid climates that typically see little precipitation. Moreover, with rising sea levels, land mass near coastal areas is at increasing risk of dangerous flooding from /other weather calamities, including intensifying hurricanes, occur. Although all infrastructure exposed to flooding is susceptible to damage [157], [158], [159], this chapter specifically addresses the threats to PV plants and illustrates the latter with case studies. Also included in this chapter are best practices to mitigate flood-related risks to PV, based on a case study in India [160].

7.2 Current practices and their limitations

Currently, reducing the risk of flooding at a PV plant falls into one of two categories: 1) Siting the plant in a low-risk area and 2) developing a robust stormwater plan that includes conduit to direct water away from the PV modules, inverters and other important structures, and into storm basins.

Both approaches, however, have limitations because they are based on historical flood patterns that may no longer be representative of projected shifts in global climate patterns, including an increase in extreme precipitation. The severity of floods in 'flood-prone' areas is likely to worsen, as evidenced by catastrophic flooding in areas historically not known to experience much flooding [161].

Insurance, while a protective strategy for many weather-related damages, is often not a straightforward solution for flooding for two reasons. One, flood-related insurance for PV is rare; and two, insurance--when it is available, is often too restrictive to be viable. Some policies, for example, require that plants be 'shut down' in anticipation of flooding and turned on only after experts have deemed it safe to do so. However, not all PV plants have a 'rapid shutdown' feature that disconnects the AC power and also individual modules from each other. For most utility-scale power plants, there are simply too many modules to enable the disconnection of individual modules in the anticipation of floods. Designing flood-resilient PV plants requires a forward-looking approach that considers realistic projections, including extreme flooding events, as predicted by most climate models.

7.3 Flood damage to PV plants

Damage caused by flooding to PV plants can be attributed to two primary stressors: 1) structural resistance to fast-flowing flood waters and 2) submergence of equipment, including electrical components, that results in waterlogging. Details of damage seen for each of these stressors (surveys were performed by the National Centre for Photovoltaic Research and Education at the Indian Institute of Technology, Bombay) is given below:

7.3.1 Resistance to fast-flowing flood waters

When structures with PV modules mounted on them are inundated by fast-flowing flood waters, the resistance of the modules to the flow of water depends on their orientation. The outcome can be catastrophic when the modules are at a high tilt angle, creating high resistance to the fast-flowing water. A fixed-tilt, south-facing plant in southern India exemplifies the risk (see Figure 29). In this case, the force of flowing water was so great that it would be futile to increase

the strength of modules/structures/ foundations to withstand this damage. The only option is to make design changes to reduce structural resistance to the fast-flowing water.

Figure 29: Damage to PV structures due to fast-flowing flood waters in southern India. Examples include destroyed modules and structures; uprooted foundations; and broken glass hit by waterborne debris.

To reduce resistance, modules should be mounted close-to-horizontal or on a tracker that has that stow capability. For example, a section of the plant at the same location as above had PV modules mounted above a canal (also known as canal-top PV) on concrete structures, but at an inclination of just 6 degrees. This section experienced the same fast flowing waters, and the modules were also submerged. Visible structural damage, however, was minimal, as seen in Figure 30, because the low-tilt angle meant less resistance to the water flow.

Figure 30: Canal-top PV system with concrete structures proved resilient to flooding because the low-tilt design posed less resistance to the fast-flowing water.

7.3.2 Submergence

All ground-mounted PV plants are vulnerable to flooding, because commercial PV modules are not designed to withstand being submerged underwater. BOS components, such as string combiner boxes (SCBs) and inverters, are even more susceptible to failure underwater. Consider that submergence can last for several days, and the water can rise several feet above the PV modules during this period, as seen in Figure 31. In addition, flood waters have high silt loads and contain contaminants that can infiltrate and soil the equipment.

Figure 31: Parts of a PV plant are submerged in 1-3 feet deep water for about two days during a flooding event.

Even when submerged, PV modules can receive sufficient light to generate high voltages at the string / SCB / inverter level. The safety hazards are significant: current leakages can immediately lead to short circuiting and fires when the water recedes, as shown in Figure 32. String-inverters / SCBs are particularly prone to catastrophic damage when short-circuiting occurs in the presence of high voltages.

Figure 32: Fire at the inverter and burned SCB at a flood-affected PV plant.

Module damage attributable to submergence falls into three categories:

- **Junction box failures**. Field studies show that modules with junction boxes that were only rated at ingress protection (IP) 65 for dust protection had burn-marks and partially melted housings, indicating a short circuit/hotspot inside the junction box. In contrast, IP67-rated junction boxes with pottant, which can withstand temporary water immersion,

had no indications of water ingress despite submergence in 1-3 feet of water for more than 48 hours. These preliminary findings suggest that the higher-rated junction boxes be specified as part of module procurement for any plant in a flood-exposed area.

- **Accelerated PID / corrosion**. Modules labeled as 'PID-resistant' did not show accelerated PID when submerged, compared to the non-submerged string. EL imaging also revealed no increase in cell cracking, although this result may depend on cell size and module architecture. However, the long-term performance ratio of these modules remains unknown.
- **Staining the glass**. A considerable amount of silt was visible on the canal-top modules after the water receded, resulting in permanent staining of the glass despite cleaning with soap water (see Figure 33). The outcome is the occurrence of permanent hotspots in the modules which will likely lead to reliability issues in the long run.

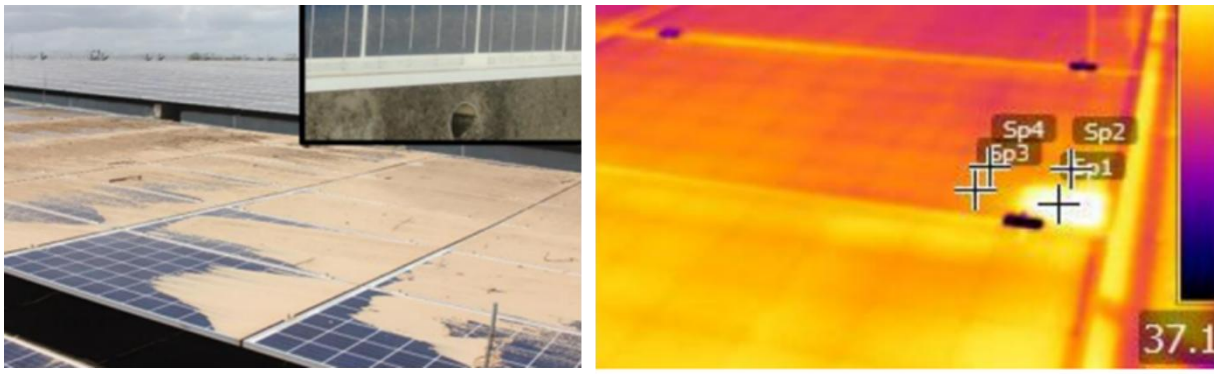

Figure 33: Silt deposition post-flooding led to permanent staining on the modules which caused hotspots.

7.4 Recommendations and key takeaways

Forecasts based on historical patterns of flooding need to be replaced with new flood forecasting systems based on advanced climate models. In addition, designs for new PV plants must reflect the growing threat of severe floods and specify tilt angles and stow strategies that lower physical resistance to fast-flowing water.

Recommended design strategies include:

- Low-tilt inclination mounting to reduce resistance, although the latter must be considered with respect to the plant's latitude and the impact on annual electricity generation for PV plants away from the equator.
- Deployment of single-axis trackers with control algorithms to stow the modules horizontally in anticipation of flooding. This approach, however, must include a robust design for the tracker posts to ensure they can withstand erosion. Concrete structures with steel bars are more robust, but not economical for large-scale applications.
- Procurement of PV modules fitted with IP67 or better-rated junction boxes.
- Procurement of IP67 or better packaging for inverters and SCBs. Note, however, that the added protection can reduce their maintainability.
- Increased ground clearance for string inverters and SCBs. Note: any impact on the shading of PV panels must be considered.

In addition, safety must always be a priority. A flooded system must be fully de-energized before it can be approached. Also, flooding can bring unexpected and potentially dangerous wildlife, including venomous snakes, into the PV plant area and personnel need to exercise extra caution while surveying the damage.

8 WILDFIRES

8.1 Overview

Wildfires are almost ubiquitous, occurring on all continents, except for Antarctica (see Figure 34). They are also increasing in frequency and intensity [162], projected to increase globally by 14% by 2030 and 50% by the end of the century [163]. In the US, climate-fire models predict a doubling of forest-fire area between 2021 and 2050, relative to the 2018-2020 season [164]. Similar increases are predicted for other continents: southern Europe could see a tenfold increase in catastrophic fires over the next decade (see Figure 35) [165]. Major fires have also been documented in Australia, Turkey, Greece, Italy, France and Spain. In 2023, Canada had its worst fire season to date, with 18.5 million hectares burned. Australia saw its average burn area increase by 350% during the period 2002-2018. The trends are clear; what remains unclear is to what extent the projected increase in wildfire activity will negatively impact the performance and reliability of PV systems, both locally and regionally.

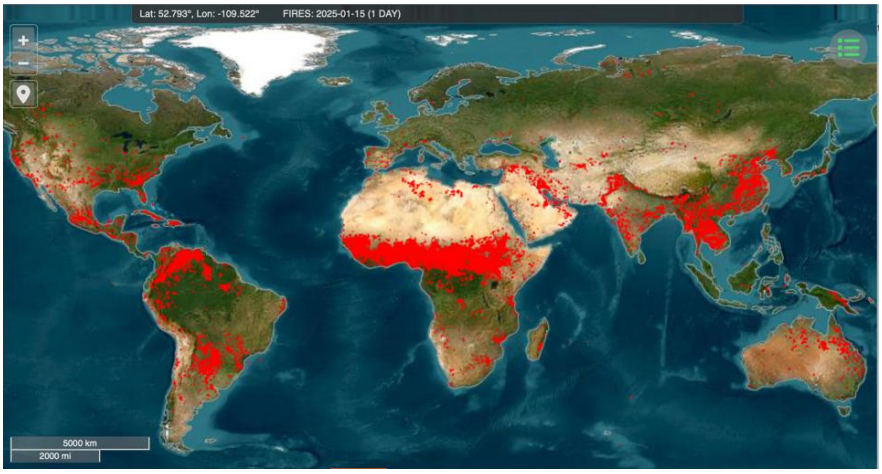

Figure 34: Prevalence of wildfires across the planet on a single day (15 Jan 2025) is depicted here, although note that most fires in South America, Africa and Asia, are deliberately set for the purposes of land clearing.

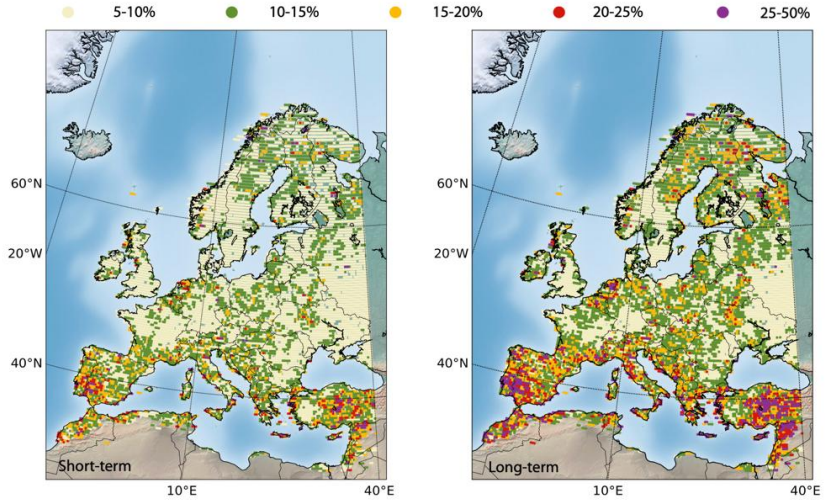

Figure 35: Increase in the probability of extreme fire events in Europe from the present (left) to the next 20 years (right). The geographic increase in fire activity overlaps with high-irradiance regions that are also experiencing an increase in PV capacity.

Fires can be triggered by human activity, both deliberate, as in the clearing of rain forests, and inadvertent, as in the careless handling of cigarettes or campfires. They can also be triggered by arc faults in an electrical network, especially if the surrounding vegetation is dry and poorly managed. But—across the board—a primary driver of wildfires is the upward trend in ambient air temperatures, notably at higher latitudes when increased temperatures are accompanied by reduced rainfall, high winds and dry vegetation.

It is important to note, however, that most wildfires occur where there is fuel, i.e., in heavily vegetated mountainous regions and forests that are not attractive to PV developers and are also far from the electricity load. But demographic data show that the gap between so-called wildlands and suburbia is narrowing, especially in the western US, increasing the risk to critical infrastructure, including PV. At the same time, the risk of PV plant-generated fires is increasing, a combination of electrical arc faults caused by malfunctioning inverters and PV connectors, and insufficient vegetation management (see Figure 36).

8.2 Wildfire risk to PV systems

Few data are available regarding the extent to which PV systems are destroyed or damaged by wildfires; data are similarly lacking for any sub-catastrophic impacts, as in the accelerated degradation of modules and other components, post smoke-exposure. Nonetheless, it is reasonable to identify three categories of impact:

- **Total or partial destruction.** Wildfire engulfs a PV power plant and destroys all or part of the plant, requiring full or partial repowering.
- **Performance losses.** Irradiance-blocking, particulate-laden smoke plumes curtail generation and also deposit particulate matter on the modules that remain once the smoke dissipates.
- **Sub-catastrophic damage**. Wildfire particulates can be caustic and electrically conductive, but their effect on the long-term reliability of PV systems is poorly documented. Given their microscopic diameter, $PM_{2.5}$ particulates are likely to penetrate the electrical balance-of-systems, e.g., connectors that are not properly torqued or maintained and left open during construction, but evidence is lacking. Similarly, little is known about how heat from an onsite fire might impact modules within a defined radius, but possibilities range from cracked cells and backsheets to encapsulant damage.

Figure 36: Onsite grass fires, likely triggered by an arc fault, generate dense smoke that can soil and penetrate a PV system, potentially creating long-term reliability risks.

8.3 Economic impacts

According to a GCube study, the number of insurance claims related to wildfire damage in PV systems is significant, although wildfire loss damages are a small fraction of those submitted for hail damage (see Figure 37). Regarding the relative cost (i.e., the proportion of total claims for each extreme weather category, the economic damages incurred by wildfires is comparable to those for hurricanes and floods, but considerably lower than for hail damage.

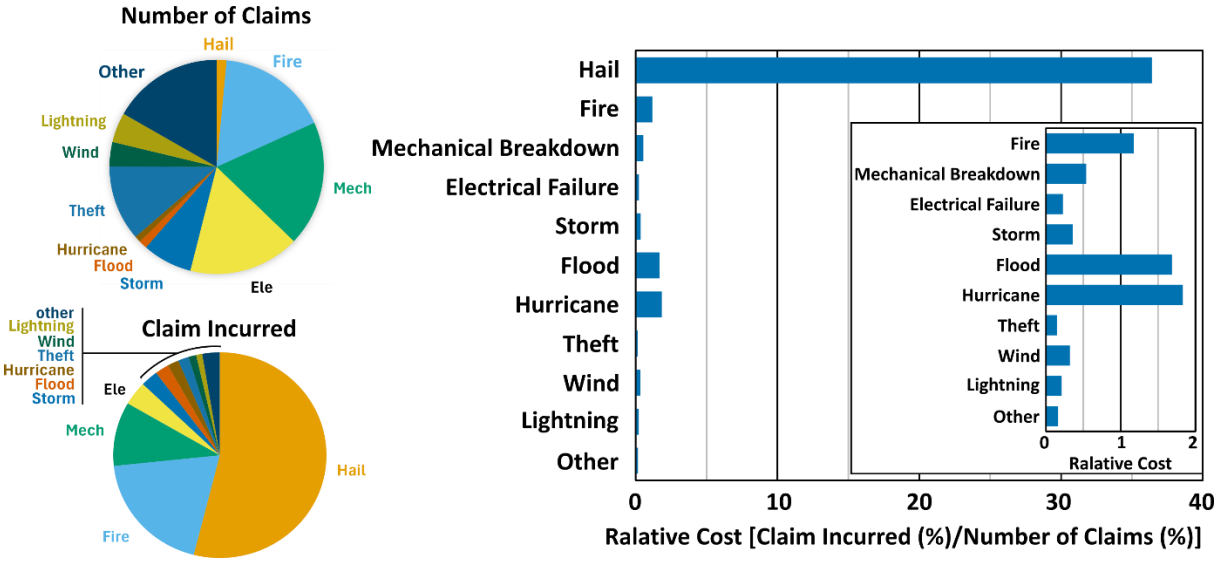

Figure 37. Number of fire claims for PV systems is high, but total costs incurred are much lower than for hail and similar to hurricanes and floods(adapted from GCube whitepaper [53]

8.4 Performance losses

Numerous studies have documented the impact of irradiance-blocking wildfire smoke on PV performance, with drops in energy production ranging as high as 40% and persisting in some cases for weeks. In 2014, a fire event in Canberra cut peak generation at a PV site by 27%. California, which has the highest wildfire activity of any US state—but also the highest installed solar capacity—has seen some of the worst solar losses attributed to wildfire smoke. When measured generation was compared with modelled generation under smoke-free conditions, smoke losses ranged from 9.4–37.8% at one site and from 9–49% at a second site [166]. The worst affected locations saw a mean loss of energy generation of 15% for the peak hour of 12 pm–1 pm [167]. Moreover, the effects are often not local. Burning forests in Sumatra, for example, reduced the energy output of a PV system in Singapore by 15–25% [168] In 2023, smoke from Canada wildfires enveloped most of the eastern US in haze, with atmospheric particulates that persisted for months.

8.4.1 New South Wales Wildfires of 2019-2020

Ford *et al.* analysed historic energy data from 170 distributed rooftop PV systems across New South Wales, correlating measured output with concentrations of airborne particulate matter ($PM_{2.5}$), the latter being an indicator of smoke density [169]. Data on particulate concentrations was collected from a network of $PM_{2.5}$ ground-measurement sensors at a distance of 5 km or less from each PV system and corrected for air mass (see Figure 38). The authors estimate the resulting total energy loss to be around 175 ± 35 GWh, equating to a worst-case financial

loss of 19 ± 4 million US dollars, with the greatest relative impact in the mornings and evenings, coinciding with periods of peak demand and value.

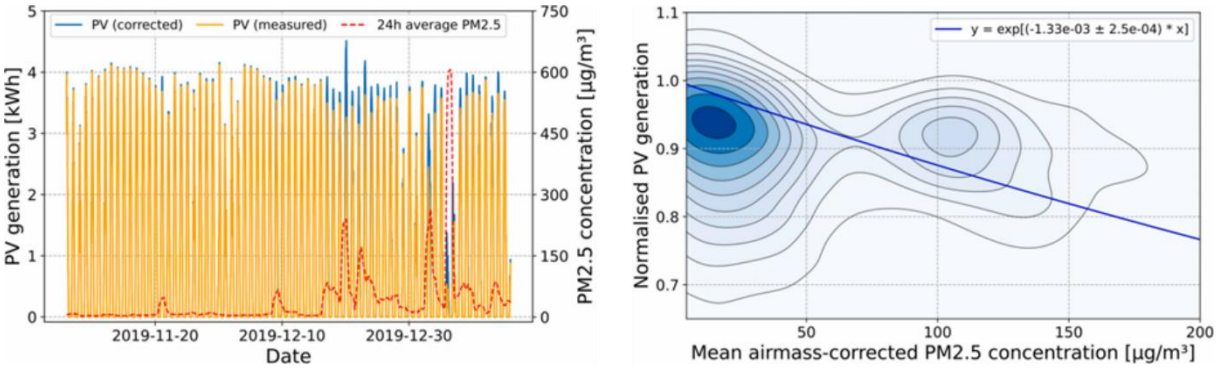

Figure 38: Impact of wildfires is depicted in the time-series graph (left) showing measured and $PM_{2.5}$-corrected PV output and $PM_{2.5}$ concentrations in Australia in 2019/2020. Spikes in $PM_{2.5}$ concentration correlate with drops in energy yields; a corresponding plot (right) indicates a strong reduction in PV generation as a function of $PM_{2.5}$ concentration. The observed mean power reduction rate for PV energy generation as a function of the $PM_{2.5}$ concentration was 13 ± 2% per 100 µg/m³ of $PM_{2.5}$, like values determined in studies conducted in Singapore and India.

8.4.2 California Wildfires of 2020

Several studies have analysed the impact of wildfire smoke on utility-scale PV generation in California during 2020, one of the worst years for wildfires on record. According to an assessment by the US Energy Information Administration, electricity generation from solar declined in California by nearly 30% on average, relative to the same month the previous year (see Figure 39).

Because smoke losses of this magnitude can impact grid stability, researchers have developed a model that combines satellite imagery and forecasts of wildfire smoke density into a tool that predicts reductions in PV electricity generation. The tool's value lies in its ability to predict seasonal capacity reductions attributable to smoke for any given location, thus supporting risk assessment studies for prospective PV sites.

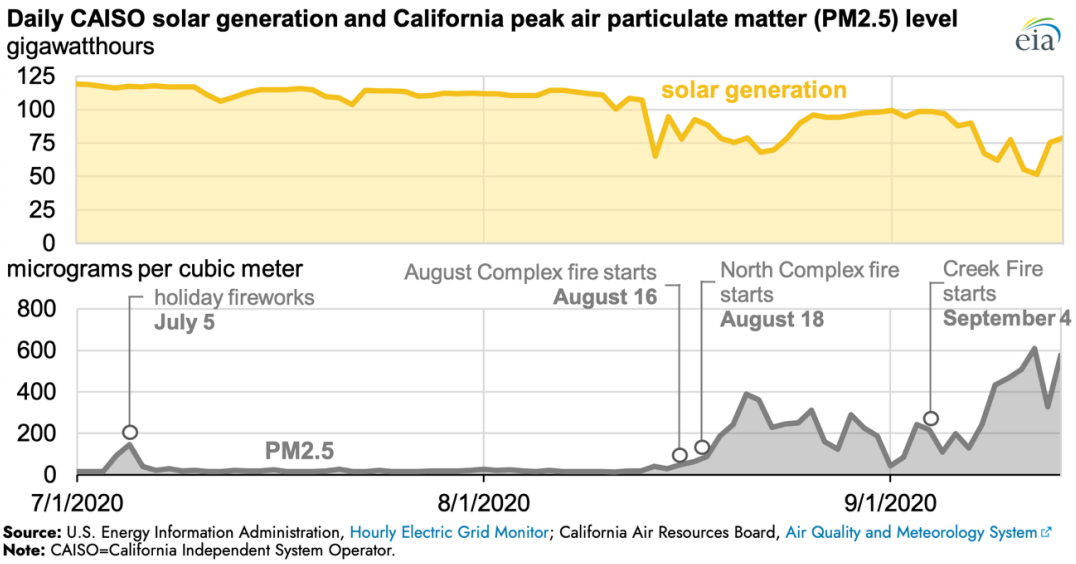

Figure 39: Daily solar generation for the peak wildfire season in California in 2020 shows a steep drop off (*top*) correlated with peaks in smoke density (*bottom*).

8.5 Mitigation strategies

Fires, which are generated onsite (typically triggered by an electrical arc fault) are sometimes categorized as wildfires. But they differ from externally generated wildfires in four ways: they are 1) less predictable; 2) relatively easy to contain; 3) are of short duration; and 4) physically destructive but have a minimal impact on irradiance blocking.

To minimize the likelihood of an onsite fire requires regular inspections of the PV plant's electrical balance of system components, including PV connectors, inverters and wiring. Mowing, or otherwise controlling, vegetation is also of high importance, especially if the vegetation has a low moisture content. Some sites deploy smoke detectors, combined with cameras, that can send an alert to grid operators, enabling rapid response.

Minimizing the risk from an uncontrolled external wildfire is more challenging and relies primarily on good siting choices based on historical fire patterns and predicted changes in precipitation. But it is also important to track fire activity that is likely to impact the plant. In the event of a descending smoke plume, operators may choose to take the plant offline; if advancing flames threaten the plant, fire suppression activities, including/ use of flam-retardants around the plant's perimeter are possible.

FUEGO is an advanced software developed by the University of California, Berkeley, to identify early forming fires based on data from multiple sources, including satellites, aerial drones with visual and thermal cameras, piloted aircraft and fire towers. In addition, several companies are developing wildfire forecasting tools based on artificial intelligence and machine learning, including Fire CNN developed at Aalto University in Finland, OroraTech in Munich, and Overstory in the Netherlands and Edgybees.

8.6 Key recommendations and takeaways

Siting PV plants in regions that are at low risk of wildfire exposure may be a challenge, given the spread of wildfire activity around the world, the growth in PV deployment and the dispersion of smoke. Minimizing a plant's proximity to pine forests with dense undergrowth is important, although the topology in those areas is not favourable to PV. Likely, however, the biggest threat to PV plants is not from physical destruction by fire but from dense, particulate-laden smoke plumes that reduce irradiance and deposit ash and soot on the modules and electrical BOS. Little can be done about the irradiance blocking but several best practices have been identified for overall risk reduction and specifically for reducing the risk of smoke exposure.

Pre-event Mitigation Strategies:

- Conduct a risk assessment prior to site development that includes analysis of historic and projected fire patterns.
- Implement a response strategy that addresses both construction and post-construction risks. For example, in a moderate-to-high risk area, all connectors should be capped until the moment of interconnection and cables should be under protective coverings to minimize 1) ingress of smoke particles into the connectors; and 2) ingress of construction dust that can lead to arc faults and onsite fires.
- Implement a vegetation management strategy that includes regular mowing and heightened vigilance under drought conditions to minimize the likelihood of onsite fires.
- Install smoke detectors at multiple locations onsite so the system can be shut down and a response team mobilized as quickly as possible. Such alarms are key to curtailing on-site fires, but they are effective only if properly monitored and if first responders can respond quickly.
- Track wildfire forecasts, which are increasingly accurate, both seasonally and geographically. Similarly, when forecasts predict that a major smoke plume is heading toward a PV plant, disconnect the plant to minimize the ingress of nanoparticles into the inverters. If the particulate concentrations are high, the shutdown should have minimal impact on energy losses given the reduced irradiance.
- Tilt trackers away from prevailing wind, to minimize front-side soiling.

Post-event Mitigation Strategies:

- Conduct visual inspections, focusing on strings that likely had high exposure to smoke, and inspect at modules for evidence of delamination, glass cracking or discoloration, backsheet soiling, and distortion/cracking/degradation of the junction box and connector housings.
- Check inverter filters for soiling, especially by carbonaceous particles.
- Implement cleaning protocols, if module glass appears excessively soiled or remains visibly soiled after a rain event
- Monitor system performance for the next 1-3 years and calculate performance ratio to identify any under-performance.

9 CONCLUSIONS

This report identifies the potential risks to PV installations from projected increases in the frequency and magnitude of extreme weather events and provides general guidelines for mitigating those risks. Our aim is to provide a repository of information and best practices for an industry where codes and standards have yet to catch up with the reality of lifetime storm exposure, from moisture ingress to structural strain on PV fasteners and tracker joints.

Fortunately, many PV plants survive extreme weather events, including high-intensity hurricanes, but others—even those adjacent to unscathed plants—are destroyed. The difference in most cases, whether the threat is from hail or floods or hurricanes, is the care taken during the design and procurement stages to ensure the construction of a well-engineered system, from depth of pilings to purlin tensile strength to bolt composition and diameter. While this report does not address the specific challenges of material fatigue and joint loosening, it does provide a broad overview of the impacts of specific storm events on PV systems and offers mitigation strategies as well as best practices.

Extreme weather events fall into two categories: 1) those that have relatively short-term impacts, e.g., tropical cyclones, convective storms (including hail), and flooding (see Table 5); and 2) those that have longer-term impacts, e.g., snow, dust storms, heatwaves, and wildfires.

Table 5: General aspects of extreme weather events.

Weather Event	Duration		Predictability Window	
Tropical Cyclones	†	1 – 2 days	‡	2 – 3 days in advance
Hailstorms	†	1 – 2 days	‡	< 24 hours in advance
Snowfalls		3 – 6 months	‡	(heavy case) several days in advance
Dust Sandstorms		several days – 1 month	‡	≤ 5 days in advance
Heat Waves		1 – 6 months		
Floods	†	several days	‡	1 day in advance
Wildfires		1 day – several months		

Dagger marks (†) in the Duration column indicate temporary events, and the double dagger marks (‡) in the Predictability Window column denote events that can be forecasted within the specified time frame.

The latter may have chronic outcomes that extend over several years, as in, repetitive stress on solar cells, or may be shorter-lived, as in snow or dust shading that can persist for weeks but eventually dissipates when it rains.

From the perspective of resilience (the ability to recover from negative impacts) and mitigation (the actions taken to reduce potential impacts), appropriate planning and design is critical and outweighs all other responses. For example, a thorough review of historical weather records, along with modelled future projections of extreme weather events for each site, should be mandatory. This step involves identifying risks based on various metrics, such as event recurrence intervals, magnitude of extreme events and the investment holding period, to ensure each is effectively considered during the design stage.

Once the threat landscape is appropriately mapped, architects, project developers and installers must make appropriate design and procurement decisions. Materials and structural

components should comply with codes and standards and be able to demonstrate survivability under a specific cluster of climatic stressors. Additionally, architects must carefully consider the terrain and geological features of the proposed installation site. For instance, when constructing a PV system on sloping terrain, the ground foundation should incorporate measures to prevent landslides from tropical cyclones or flooding. Key recommendations for mitigating the impacts of various weather events are summarized in Table 6 below.

Table 6: Design recommendations to mitigate the impacts of respective weather events.

Weather Event	Recommendations (Brief summary; detailed guidance provided in respective chapters)
Tropical Cyclones	- Design robust mounting structures to withstand strong wind loads. - Use PV modules resistant to strong wind loads and heavy rain.
Hailstorms	- Incorporate an adequate stowing system into the tracker. - Use PV modules with thicker front glass for enhanced durability.
Snow	- Design systems with high tilt-angles (if fixed tilt) advanced stow strategies for snow (if trackers) and high ground clearance, - Select PV modules resistant to heavy snow loads (thicker front glass and heavier frames relative to surface area). - Consider PV modules with snow-removal properties (e.g., frameless designs).
Dust Sandstorms	- Incorporate preventive designs to reduce soil accumulation (e.g., tracker systems that can tilt at high angles). - Compare performance of anti-soiling coatings against predicted soiling losses. - Develop performance- and cost-effective cleaning protocols.
Heat Waves	- Install inverters in cool, shaded locations or add covers for shade. - Select PV modules with a low temperature coefficient.
Floods	- Install tracker systems that can move quickly to a horizontal stow position to reduce physical resistance to flowing water. - Use robust mounting structures with high ground clearance for inverters and string combiner boxes. - Install highly waterproof containers (IP67) for inverters and combiner boxes.
Wildfires	- Have a rapid response strategy in place, including shutdown protocols - Conduct post-fire inspections and monitor subsequently for signs of module and connector degradation.

In addition, site owners/operators should retain various documents, including those related to capacity testing and energy production, module and component specifications, and

commissioning. Any EL and/or IR images, as well as documentation of visual inspections and I-V measurements, should be preserved to establish a baseline against which the storm-impacted system can be compared.

Electrical performance data also serves as a fundamental basis for assessing the impacts of extreme weather events and any accelerated increase in degradation. Combining electrical performance data with weather conditions, such as temperature, irradiation, and wind speed, provides time-series data that can help identify weather-inflicted damage. But the site owner and maintenance personnel must recognize the importance of acquiring and maintaining such data.

Proactive maintenance protocols are also critical and should reflect the predictability of the threat. For instance, a torque audit of fasteners and the removal of onsite debris, which could become airborne, should be performed prior to a high wind event.

If damage from extreme weather does occur, remediation should begin as soon as possible. Activities include 1) ensuring the safety of the site by disconnecting it from the grid and opening all breakers; 2) conducting electrical and mechanical inspections of the affected PV system; and 3) leaving damage *in situ*, pending notification of the insurance company and any follow-on inspections. All damaged PV modules and electrical components should be replaced prior to re-energization. Modules that are heavily soiled should be cleaned; electrical components should be IR-imaged; and electrical cables inspected and remounted, as needed. After dust and sandstorm events, the surfaces of PV modules and the electrical parts both inside and outside of SCBs and inverter enclosures must be cleaned.

Long-term O&M protocols are also of paramount importance. Defects that are not fully addressed during the post-storm restoration phase are likely to be exacerbated by environmental factors such as temperature, wind, and moisture. Therefore, continuous monitoring of power generation for restored PV systems is crucial to establish their ongoing health and efficiency. If a significant reduction in power output occurs, the owner will then have the data needed to decide on the next steps, including system refurbishment.

In summary, the authors of this report believe that by adhering to the above recommendations, PV systems in most parts of the world can be made resilient to most severe weather threats and remain a robust and reliable source of electricity generation.

REFERENCES

[1] Intergovernmental Panel on Climate Change (IPCC), "Climate change 2021 – The physical science basis," Cambridge University Press, Jul. 2023. doi: 10.1017/9781009157896.

[2] Q. Wang, K. Liu, W. Xie, T. Ali, J. Wu, and M. Wang, "Photovoltaic installations are extensively deployed in areas at risk of extremely low production," *Commun. Earth Environ.*, vol. 5, no. 1, p. 752, Dec. 2024, doi: 10.1038/s43247-024-01932-4.

[3] NOAA National Centers for Environmental Information (NCEI), "U.S. billion-dollar weather and climate disasters: Time series." Accessed: Apr. 14, 2025. [Online]. Available: https://www.ncei.noaa.gov/access/billions/time-series

[4] A. Tamizi and I. R. Young, "A dataset of global tropical cyclone wind and surface wave measurements from buoy and satellite platforms," *Sci. Data*, vol. 11, no. 1, p. 106, Jan. 2024, doi: 10.1038/s41597-024-02955-4.

[5] M. F. Wehner and J. P. Kossin, "The growing inadequacy of an open-ended Saffir–Simpson hurricane wind scale in a warming world," *Proc. Natl. Acad. Sci.*, vol. 121, no. 7, p. e2308901121, Feb. 2024, doi: 10.1073/PNAS.2308901121.

[6] NOAA National Centers for Environmental Information (NCEI), "U.S. billion-dollar weather and climate disasters: Disaster cost and frequency." Accessed: Apr. 11, 2025. [Online]. Available: https://www.ncei.noaa.gov/access/billions/mapping

[7] K. S. Fujita *et al.*, "Georectified polygon database of ground-mounted large-scale solar photovoltaic sites in the United States," *Sci. Data*, vol. 10, no. 1, p. 760, Nov. 2023, doi: 10.1038/s41597-023-02644-8.

[8] Lawrence Berkeley National Laboratory and U.S. Giological Survey, "United States large-scale solar photovoltaic database." Accessed: Apr. 11, 2025. [Online]. Available: https://energy.usgs.gov/uspvdb/viewer/#3/41.77/-85.57

[9] J. Gifford, "Long read: What broke at Oakey – PV magazine Australia," PV Magazine. Accessed: Mar. 26, 2024. [Online]. Available: https://www.pv-magazine-australia.com/2019/12/07/long-read-what-broke-at-oakey/

[10] U. Jahn *et al.*, *Guidelines for operation and maintenance of photovoltaic power plants in different climates*. Paris, France: International Energy Agency, 2022. [Online]. Available: https://iea-pvps.org/key-topics/guidelines-for-operation-and-maintenance-of-photovoltaic-power-plants-in-different-climates/

[11] W. Cole, D. Greer, and K. Lamb, "The potential for using local PV to meet critical loads during hurricanes," *Sol. Energy*, vol. 205, no. February, pp. 37–43, Jul. 2020, doi: 10.1016/j.solener.2020.04.094.

[12] N. D. Jackson and T. Gunda, "Evaluation of extreme weather impacts on utility-scale photovoltaic plant performance in the United States," *Appl. Energy*, vol. 302, p. 117508, Nov. 2021, doi: 10.1016/j.apenergy.2021.117508.

[13] D. C. Jordan, K. Perry, R. White, and C. Deline, "Extreme weather and PV performance," *IEEE J. Photovoltaics*, vol. 13, no. 6, pp. 830–835, Nov. 2023, doi: 10.1109/JPHOTOV.2023.3304357.

[14] M. Yamazaki, "Guidelines for the design and construction of photovoltaic power system (in Japanese)." Accessed: Nov. 25, 2024. [Online]. Available: https://www.jpea.gr.jp/wp-

content/uploads/211224_2_NEDO.pdf

[15] "Study results: Understanding photovoltaic power generation facility insurance accident trends for businesses (in Japanese)," General Insurance Association of Japan, 2024. [Online]. Available: https://www.sonpo.or.jp/news/notice/2023/pdf/240209_report.pdf

[16] GreenValley International, "Solar energy - Intelligent inspection project using LiDAR and point cloud data." Accessed: Nov. 25, 2024. [Online]. Available: https://www.greenvalleyintl.com/power-line-case-studies/solar-energy-intelligent-inspection-project.html

[17] "Severe weather resilience in solar photovoltaic system design." Accessed: Mar. 26, 2024. [Online]. Available: https://www.energy.gov/femp/severe-weather-resilience-solar-photovoltaic-system-design

[18] J. Elsworth *et al.*, "Toward solar photovoltaic storm resilience: Learning from hurricane loss and rebuilding better," Federal Energy Management Program, Washington DC, USA, 2023. Accessed: Mar. 26, 2024. [Online]. Available: https://www.energy.gov/femp/articles/toward-solar-photovoltaic-storm-resilience-learning-hurricane-loss-and-rebuilding

[19] G. Robinson *et al.*, "PV system owner's guide to identifying, Assessing, and addressing weather vulnerabilities, risks, and impacts," Federal Energy Management Program, Washington DC, USA, 2021. Accessed: Mar. 26, 2024. [Online]. Available: https://www.energy.gov/femp/articles/pv-system-owners-guide-identifying-assessing-and-addressing-weather-vulnerabilities

[20] "Preparing solar photovoltaic systems against storms," National Renewable Energy Laboratory (NREL), Golden, CO (United States), 2022. Accessed: Oct. 18, 2022. [Online]. Available: https://www.osti.gov/biblio/1873500

[21] FMEA Mitigation Assessment Team, "Hurricanes Irma and Maria in the U.S. Virgin islands: Building performance observations, recommendations, and technical guidance," Federal Emergency Management Agency, Washington DC, USA, 2018. [Online]. Available: https://www.fema.gov/media-library/assets/documents/170486

[22] FMEA Mitigation Assessment Team, "Rooftop solar panel attachment: Design, installation, and maintenance," Federal Emergency Management Agency, Washington DC, USA, 2018. [Online]. Available: https://www.fema.gov/media-library-data/1535554011182-e061c2804fab7556ec848ffc091d6487/USVI-RA5RooftopSolarPanelAttachment_finalv3_508.pdf

[23] "Solar photovoltaic systems in hurricanes and other severe weather," Federal Energy Management Program, Washington DC, USA, Aug. 2018. Accessed: Mar. 26, 2024. [Online]. Available: https://www.osti.gov/biblio/1468519

[24] C. Burgess and J. Goodman, "Solar under storm select best practices for resilient ground-mount PV systems with hurricane exposure," Rocky Mountain Institute, Basalt, CO. USA, 2018. [Online]. Available: https://rmi.org/wp-content/uploads/2018/06/Islands_SolarUnderStorm_Report_digitalJune122018.pdf

[25] J. Elsworth and O. Van Geet, "Solar photovoltaics in severe weather: Cost considerations for storm hardening PV systems for resilience," National Renewable Energy Laboratory (NREL), Golden, CO (United States), Jun. 2020. doi: 10.2172/1659785.

[26] C. Burgess, S. Detweiler, C. Needham, and F. Oudheusden, "Solar under storm Part II: Select best practices for resilient roof-mount PV systems with hurricane exposure,"

Rocky Mountain Institute, Basalt, CO. USA, 2020. [Online]. Available: https://rmi.org/solar-under-storm-part-ii-designing-hurricane-resilient-pv-systems/

[27] C. Burgess, J. Locke, and L. Stone, “Solar under storm for policymakers: Select best practices for resilient photovoltaic systems for small island developing states,” Rocky Mountain Institute, Basalt, CO. USA, 2020. Accessed: Mar. 26, 2024. [Online]. Available: https://rmi.org/solar-under-storm-for-policymakers/

[28] “Cyclone and storm tide resilient building guidance for Queensland Homes | Queensland reconstruction authority,” Queensland Reconstruction Authority, 2019. Accessed: Mar. 26, 2024. [Online]. Available: https://www.qra.qld.gov.au/resilient-homes/cyclone-and-storm-tide-resilient-building-guidance-queensland-homes

[29] A. Roedel and K. Whitfield, “White paper: Mitigating extreme weather risk Part 1: Understanding how differentiated design and control strategies unlock new opportunities for solar development,” Nextracker, 2020. Accessed: Mar. 26, 2024. [Online]. Available: https://info.nextracker.com/mitigating-extreme-weather-risk

[30] A. Roedel and J. Butcher, “Nextracker white paper: Mitigating extreme weather risk Part 2: Surviving high-wind events and dynamic-wind effects with differentiated solar project design and control strategies,” Nextacker, 2021. Accessed: Mar. 26, 2024. [Online]. Available: https://info.nextracker.com/mitigating-extreme-weather-risk-part-2

[31] “Property loss prevention data sheets 1-15: Roof-mounted solar photovoltaic panels,” FM Global, 2024. [Online]. Available: https://www.fmglobal.com/research-and-resources/fm-global-data-sheets

[32] “Property loss prevention data sheets 7-106: Ground-mounted solar photovoltaic power,” FM Global, 2024. [Online]. Available: https://www.fmglobal.com/research-and-resources/fm-global-data-sheets

[33] “Minimum design loads and associated criteria for buildings and other structures (ASCE/SEI 7-22),” American Society of Civil Engineers, 2021. [Online]. Available: https://www.asce.org/asce-7/

[34] SEAOC Solar Photovoltaic Systems Committee, “Wind design for solar arrays (PV2-2017),” Structural Engineers Association of California (SEAOC), Sacramento, CA USA, 2017.

[35] “Eurocode 1. Actions on structures - General actions - Wind actions (EN 1991-1-4/AC),” European Committee for Standardization (CEN), 2010. Accessed: Mar. 26, 2024. [Online]. Available: https://knowledge.bsigroup.com/products/eurocode-1-actions-on-structures-general-actions-wind-actions?version=standard

[36] “Structural design actions, Part 2: Wind actions (AS/NZS 1170.2:2021),” Standards New Zealand and Standards Australia, 2021. [Online]. Available: https://www.standards.org.au/standards-catalogue/standard-details?designation=as-nzs-1170-2-2021

[37] “Load dode for the design of building structures (GB 50009-2012),” Ministry of Housing and Urban-Rural Construction of the People’s Republic of China, 2012. [Online]. Available: https://www.chinesestandard.net/AMP/PDF.amp.aspx/GB50009-2012

[38] “Evaluation guide for design wind loads of photovoltaic systems (CNS-16189:2022),” Bureau of Standards, Metrology and Inspection of the Ministry of Economic Affairs, Repablic of Chana (Taiwan), 2022. [Online]. Available: https://cns-standards.org/CNS_standard_cn.asp?code=CNS 16189

[39] "Interpretation for 'Ministerial order on technical standards for solar photovoltaic power generation facilities' (in Japanese)," Ministry of Economy, Trade and Industry, Japan, 2021. [Online]. Available: https://www.meti.go.jp/policy/safety_security/industrial_safety/oshirase/2021/04/20210401-05.pdf

[40] "Load design guide on structures for photovoltaic array (JIS C 8955)," Japanese Standards Association, 2017. [Online]. Available: https://store.accuristech.com/standards/jis-c-8955-2017?product_id=1984692

[41] "Design guidelines for ground-mounted solar photovoltaic power systems (in Japanese)," New Energy and Industrial Technology Development Organization (NEDO), Japan Photovoltaic Energy Association (JPEA), and Okuji Kensan Co., LTD., 2019. [Online]. Available: https://www.nedo.go.jp/content/100895022.pdf

[42] *Design and construction guidelines for sloped-terrestrial mounted solar photovoltaic power systems (in Japanese)*. New Energy and Industrial Technology Development Organization (NEDO),Japan, 2023. [Online]. Available: https://www.nedo.go.jp/content/100960314.pdf

[43] *Design and construction guidelines for floating solar photovoltaic power systems (in Japanese)*. New Energy and Industrial Technology Development Organization (NEDO),Japan, 2023. [Online]. Available: https://www.nedo.go.jp/content/100960316.pdf

[44] "Design and construction guidelines for agrovoltaic systems (in Japanese)," New Energy and Industrial Technology Development Organization (NEDO), Japan, 2023. [Online]. Available: https://www.nedo.go.jp/content/100960315.pdf

[45] "Evaluation of photovoltaic (PV) module to mounting structure interface (IEC TS 63348)," Intenational Electrotechnical Commission. [Online]. Available: https://www.iec.ch/dyn/www/f?p=103:38:59822593875::::FSP_ORG_ID,FSP_APEX_PAGE,FSP_PROJECT_ID:1276,23,104319

[46] J. T. Allen, "Toward a global understanding of severe convective environments." Accessed: Nov. 21, 2024. [Online]. Available: https://people.se.cmich.edu/allen4jt/allen_currentprojects_globalstorms.html

[47] R. Kennedy, "Over half of solar facility loss claim costs are due to hail damage," PV magazine International. [Online]. Available: https://pv-magazine-usa.com/2023/12/06/over-half-of-solar-facility-loss-claim-costs-are-due-to-hail-damage/

[48] National Oceanic and Atmospheric Association (NOAA), "Weather glossary." Accessed: Nov. 21, 2024. [Online]. Available: https://www.noaa.gov/jetstream/appendix/weather-glossary

[49] M. Taszarek, J. T. Allen, M. Marchio, and H. E. Brooks, "Global climatology and trends in convective environments from ERA5 and rawinsonde data," *npj Clim. Atmos. Sci.*, vol. 4, no. 1, p. 35, Jun. 2021, doi: 10.1038/s41612-021-00190-x.

[50] J. T. Allen *et al.*, "Understanding hail in the earth system," *Rev. Geophys.*, vol. 58, no. 1, Mar. 2020, doi: 10.1029/2019RG000665.

[51] A. R. Crimmins, C. W. Avery, D. R. Easterling, K. E. Kunkel, B. C. Stewart, and T. K. Maycock, Eds., "Fifth national climate assessment," Washington, DC, 2023. doi: 10.7930/NCA5.2023.

[52] Munich Re., “Hail – An underestimated and growing risk: Compelling reasons to take action.” Accessed: Nov. 21, 2024. [Online]. Available: https://www.munichre.com/en/insights/natural-disaster-and-climate-change/hail.html

[53] GCube Insurance, “HAIL NO! Defending solar against nature’s cold assault,” 2023. [Online]. Available: https://gcube-insurance.com/Insights/Reports/Hail-No

[54] NOAA National Severe Storms Laboratory, “Severe weather 101 - Hail.” Accessed: Nov. 21, 2024. [Online]. Available: https://www.nssl.noaa.gov/education/svrwx101/hail/

[55] T. Teule, M. Appeldoorn, P. Bosma, L. Sprenger, E. Koks, and H. de Moel, “The vulnerability of solar panels to hail,” Dec. 2019. Accessed: Nov. 21, 2024. [Online]. Available: https://research.vu.nl/en/publications/the-vulnerability-of-solar-panels-to-hail

[56] A. Sagar, “Texas hailstorm set to generate $70mn–$80mn solar loss,” Insurance Insider. Accessed: Nov. 22, 2024. [Online]. Available: https://www.insuranceinsider.com/article/2876gerfr59h81ziaca2o/texas-hailstorm-set-to-generate-70mn-80mn-solar-loss?zephr_sso_ott=Ui7BBs

[57] B. Taylor, J. Sedgwick, and M. Perron, “How technology is protecting solar farms against extreme weather.” Accessed: Nov. 22, 2024. [Online]. Available: https://vimeo.com/881850247/4dc43fc4be

[58] T. Sylvia, “Extreme weather is causing solar insurance premiums to explode,” PV magazine. Accessed: Nov. 22, 2024. [Online]. Available: https://pv-magazine-usa.com/2020/12/14/extreme-weather-is-causing-solar-insurance-premiums-to-explode/

[59] J. Kopp, K. Schröer, C. Schwierz, A. Hering, U. Germann, and O. Martius, “The summer 2021 Switzerland hailstorms: weather situation, major impacts and unique -observational data,” *Weather*, vol. 78, no. 7, pp. 184–191, Jul. 2023, doi: 10.1002/wea.4306.

[60] E. Bamberger, “Auswertung von Feldmessungen zu Hagelschäden an PV-Modulen (Evaluation of field measurements on hail damage to PV modules),” in *Schweizer Photovoltaik-Tagung*, 2024. [Online]. Available: https://www.swissolar.ch/pv-tagung/pvt24/praesentationen/pvt24_session-5a.zip

[61] J. Scully, “Solar module testing ‘inadequate to account for rising severity of extreme weather’, report claims,” PV Tech. Accessed: Nov. 22, 2024. [Online]. Available: https://www.pv-tech.org/solar-module-testing-inadequate-to-account-for-rising-severity-of-extreme-weather-report-claims/

[62] J. H. Cain and D. Banks, “Wind loads on utility scale solar PV power plants,” in *2015 SEAOC Convention*, 2015. [Online]. Available: https://www.cppwind.com/wp-content/uploads/2020/12/Wind-Loads-on-Utility-Scale-Solar-PV-Power-Plants_DBanks_2015.pdf

[63] C. Rohr, P. A. Bourke, and D. Banks, “Torsional instability of single-axis solar tracking systems,” in *14th International Conference on Wind Engineering*, Porto Alegre, Brazil, 2015. [Online]. Available: https://cppwind.cachecloud.com/wp-content/uploads/2020/12/Torsional-Instability-of-Single-Axis-Solar-Tracking-Systems-Rohr-Bourke-Banks-2015.pdf

[64] “Hail damage mitigation for solar photovoltaic systems,” Federal Energy Management Program. [Online]. Available: https://www.energy.gov/femp/hail-damage-mitigation-solar-photovoltaic-systems

[65] T. Kropp, M. Schubert, and J. H. Werner, “Quantitative prediction of power loss for damaged photovoltaic modules using electroluminescence,” *Energies*, vol. 11, no. 5, p. 1172, May 2018, doi: 10.3390/en11051172.

[66] P. Bostock, K. Elser, and J. Previtali, “Best practices for hail stow of single-axis tracker-mounted solar projects,” VDE America, 2024. [Online]. Available: https://www.vde.com/resource/blob/2302740/4deff2e307bc9e60c300db76ec070b51/hail-stow-tech-memo-pdf-data.pdf

[67] J. Sedgwick, “Navigating hailstorms,” PV Magazine. Accessed: Nov. 22, 2024. [Online]. Available: https://www.pv-magazine.com/2022/12/24/weekend-read-navigating-hailstorms/

[68] P. Bostock, “Hail Cat: Presenting a method to identify, quantify, and mitigate hail risk,” in *PV Reliability Workshop 2024*, Lakewood, CO. USA: National Renewable Energy Laboratory (NREL), 2024, p. 319. [Online]. Available: https://www.nrel.gov/docs/fy25osti/90586.pdf

[69] S. Bhavsar and N. Shiradkar, “Data-driven approach for quantifying the risk of hail impact on photovoltaic plants,” in *2022 IEEE International Conference on Emerging Electronics (ICEE)*, IEEE, Dec. 2022, pp. 1–4. doi: 10.1109/ICEE56203.2022.10117841.

[70] C. Kedir, “Modules made with tempered glass are approximately 2x asresilient to hail impacts as those with heat-strengthened glass,” in *Solar Risk Assessment 2023*, kWh Analytics, 2023, p. 7. [Online]. Available: https://www.kwhanalytics.com/solar-risk-assessment

[71] “Hail resistance testing and analysis of results: Evaluation of Nextracker hail stow,” RETC, 2020.

[72] CFPA Eurpoe, “Protection against hail damage,” 2022. Accessed: Nov. 25, 2024. [Online]. Available: https://cfpa-e.eu/app/uploads/2022/07/Guideline_Hail20230301a-1.pdf

[73] “Understanding the hail durability test (HDT) program,” RETC, 2022. Accessed: Nov. 24, 2024. [Online]. Available: https://retc-ca.com/download-2022-pvmi

[74] A. Roedel and S. Upfill-Brown, “Designing for the wind: Using dynamic wind analysis and protective stow strategies to lower solar tracker lifetime costs,” Nextracker, 2018. Accessed: Nov. 24, 2024. [Online]. Available: https://info.nextracker.com/nextracker-designing-for-the-wind

[75] “From random to repeatable: Inside the hail stress sequence for PVEL’s PV Module product qualification program,” PVEL, 2021. [Online]. Available: https://www.pvel.com/wp-content/uploads/PVEL_White-Paper_Hail-Stress-Sequence-for-PV-Modules.pdf

[76] A. Heymsfield, M. Szakáll, A. Jost, I. Giammanco, and R. Wright, “A comprehensive observational study of graupel and hail terminal velocity, mass flux, and kinetic energy,” *J. Atmos. Sci.*, vol. 75, no. 11, pp. 3861–3885, Nov. 2018, doi: 10.1175/JAS-D-18-0035.1.

[77] N. Thompson, “Proactive hail stow program can reduce property insurance premiums,” kWh Analytics, 2023. Accessed: Nov. 25, 2024. [Online]. Available: https://www.kwhanalytics.com/solar-risk-assessment

[78] IEA PVPS Task 13 Sub-Task 3.2 Team, “Guideline for the optimization of PV system

key performance indicators," 2025.

[79] "Terrestrial photovoltaic (PV) modules – Design qualification and type approval – Part 2: Test procedures (IEC 61215-2)," International Electrotechnical Commission, Geneva, Switzerland, 2021. [Online]. Available: https://webstore.iec.ch/publication/61350

[80] T. Tanahashi, T. Chiba, S. Adachi, Y. Tsuno, K. Ikeda, and T. Oozeki, "Mitigation of heavy snow load on PV Modules installed in a snowy region," in *2023 PV Reliability Workshop*, 2023, p. 76. [Online]. Available: https://www.nrel.gov/docs/fy24osti/87918.pdf

[81] I. Frimannslund, T. Thiis, A. Aalberg, and B. Thorud, "Polar solar power plants – Investigating the potential and the design challenges," *Sol. Energy*, vol. 224, pp. 35–42, Aug. 2021, doi: 10.1016/j.solener.2021.05.069.

[82] I. Frimannslund, T. Thiis, A. D. Ferreira, and B. Thorud, "Impact of solar power plant design parameters on snowdrift accumulation and energy yield," *Cold Reg. Sci. Technol.*, vol. 201, p. 103613, Sep. 2022, doi: 10.1016/J.COLDREGIONS.2022.103613.

[83] A. Brooks, S. Gamble, J. Dale, and M. Gibbons, "Determining snow loads on buildings with solar arrays," in *CSCE 2014 4th International Structural Specialty Conference*, Halifax, NS: Canadian Society for Civil Engineering, 2014, p. CST-49.

[84] M. Lindh, A. Granlund, J. Sundström, M. Axelson, and A. M. Petersson, "Effekter och hantering av snölaster vid takmonterade solelanläggningar (Effects and management of snow loads in roof-mounted solar installations)," Swedish Energy Agency, 2024. [Online]. Available: https://www.e2b2.se/media/nv0jrg2h/slutrapport-p2018-016202.pdf

[85] A. Fang, "Keeping up with growing demand," *PV Magazine*, 2022. Accessed: Nov. 20, 2024. [Online]. Available: https://www.pv-magazine.com/magazine-archive/keeping-up-with-growing-demand/

[86] T. Sylvia, "On track for cost reduction," *PV Magazine*, 2022. Accessed: Nov. 20, 2024. [Online]. Available: https://www.pv-magazine.com/magazine-archive/on-track-for-cost-reduction/

[87] L. Burnham, D. Riley, B. King, W. Snyder, K. Santistevan, and P. W. Dice, "Module reliability in winter: field analysis of deflection and cell cracking across multiple module architectures," in *2023 IEEE 50th Photovoltaic Specialists Conference (PVSC)*, IEEE, Jun. 2023, pp. 1–3. doi: 10.1109/PVSC48320.2023.10359901.

[88] L. Papargyri *et al.*, "Modelling and experimental investigations of microcracks in crystalline silicon photovoltaics: A review," *Renew. Energy*, vol. 145, pp. 2387–2408, Jan. 2020, doi: 10.1016/j.renene.2019.07.138.

[89] E. J. Schneller, H. Seigneur, J. Lincoln, and A. M. Gabor, "The impact of cold temperature exposure in mechanical durability testing of PV modules," in *2019 IEEE 46th Photovoltaic Specialists Conference (PVSC)*, IEEE, Jun. 2019, pp. 1521–1524. doi: 10.1109/PVSC40753.2019.8980533.

[90] H. Seigneur *et al.*, "Microcrack formation in silicon solar cells during cold temperatures," in *2019 IEEE 46th Photovoltaic Specialists Conference (PVSC)*, IEEE, Jun. 2019, pp. 1–6. doi: 10.1109/PVSC40753.2019.9198968.

[91] M. Köntges, J. Lin, and L. Bruckman, "Degradation and failure modes in new photovoltaic cell and module technologies," International Energy Agency, Paris, France, 2025. doi: 10.69766/ATBD2730.

[92] National Institute of Technology and Evaluation (NITE), “Surge in Snow-Induced Damage to Solar Panels in Heavy Snow Years – Equivalent to Power Supply for 75,000 Households Over Four Years (in Japanese).” Accessed: Apr. 18, 2025. [Online]. Available: https://www.nite.go.jp/gcet/tso/prs230126.html

[93] National Institute of Technology and Evaluation (NITE), “Sharp Increase in Solar Panel and Related Equipment Damage in Heavy Snow Years – Severe Impact Even on Small-Scale Power Systems (in Japanese).” [Online]. Available: https://www.nite.go.jp/gcet/tso/prs231222.html

[94] E. Bellini, “Heating solar panels to clear snow,” PV Magazine. [Online]. Available: https://www.pv-magazine.com/2020/03/18/heating-solar-panels-to-clear-snow/

[95] B. L. Aarseth *et al.*, “Mitigating snow on rooftop PV systems for higher energy yield and safer roofs,” in *35th European Photovoltaic Solar Energy Conference and Exhibition*, 2018, pp. 1630–1635. doi: 10.4229/35thEUPVSEC20182018-6CO.3.5.

[96] L. Li *et al.*, “Enabling renewable energy technologies in harsh climates with ultra-efficient electro-thermal desnowing, defrosting, and deicing,” *Adv. Funct. Mater.*, vol. 32, no. 31, p. 2201521, Aug. 2022, doi: 10.1002/ADFM.202201521.

[97] A. Granlund, M. Lindh, T. Vikberg, and A. M. Peterson, “Evaluation of snow removal methods for rooftop photovoltaics,” in *8th World Conference on Photovoltaic Energy Conversion*, 2022, pp. 1122–1128. doi: 10.4229/WCPEC-82022-4DO.4.6.

[98] A. Chutani, A. Dyreson, and L. Burnham, “Snow loss estimation for photovoltaic single-axis tracker systems,” in *IEEE 53rd Photovoltaic Specialist Conference (PVSC)*, 2025.

[99] A. Dhyani, C. Pike, J. L. Braid, E. Whitney, L. Burnham, and A. Tuteja, “Facilitating large-scale snow shedding from in-field solar arrays using icephobic surfaces with low-interfacial toughness,” *Adv. Mater. Technol.*, p. 2101032, Nov. 2021, doi: 10.1002/admt.202101032.

[100] K. Sullivan, “Photovoltaic panels catch the sun despite the snow,” *Sandia Lab News*, vol. 74, no. 13, p. 10, 2022. Accessed: Nov. 21, 2024. [Online]. Available: https://www.sandia.gov/app/uploads/sites/81/2022/07/labnews_07-14-22.pdf

[101] B. Mohammadian, N. Namdari, A. H. Abou Yassine, J. Heil, R. Rizvi, and H. Sojoudi, “Interfacial phenomena in snow from its formation to accumulation and shedding,” *Adv. Colloid Interface Sci.*, vol. 294, p. 102480, Aug. 2021, doi: 10.1016/J.CIS.2021.102480.

[102] D. Riley, L. Burnham, B. Walker, and J. M. Pearce, “Differences in snow shedding in photovoltaic systems with framed and frameless modules,” in *2019 IEEE 46th Photovoltaic Specialists Conference (PVSC)*, IEEE, Jun. 2019, pp. 0558–0561. doi: 10.1109/PVSC40753.2019.8981389.

[103] R. W. Andrews and J. M. Pearce, “The effect of spectral albedo on amorphous silicon and crystalline silicon solar photovoltaic device performance,” *Sol. Energy*, vol. 91, pp. 233–241, May 2013, doi: 10.1016/j.solener.2013.01.030.

[104] M. P. Brennan, A. L. Abramase, R. W. Andrews, and J. M. Pearce, “Effects of spectral albedo on solar photovoltaic devices,” *Sol. Energy Mater. Sol. Cells*, vol. 124, pp. 111–116, May 2014, doi: 10.1016/j.solmat.2014.01.046.

[105] K. S. Hayibo, A. Petsiuk, P. Mayville, L. Brown, and J. M. Pearce, “Monofacial vs bifacial solar photovoltaic systems in snowy environments,” *Renew. Energy*, vol. 193, pp. 657–668, Jun. 2022, doi: 10.1016/j.renene.2022.05.050.

[106] L. Burnham, D. Riley, B. Walker, and J. M. Pearce, “Performance of bifacial photovoltaic

modules on a dual-axis tracker in a high-latitude, high-albedo environment," in *2019 IEEE 46th Photovoltaic Specialists Conference (PVSC)*, IEEE, Jun. 2019, pp. 1320–1327. doi: 10.1109/PVSC40753.2019.8980964.

[107] M. Ross and J. Royer, "The effects of cold climates on photovoltaic systems," in *Photovoltaics in Cold Climates*, M. Rossol and J. Royer, Eds., London, UK: James and James Science Publishers, Ltd., 1999, pp. 39–66. [Online]. Available: http://www.rerinfo.ca/english/publications/pubBook1999PVinCC.html

[108] J. L. Braid, D. Riley, J. M. Pearce, and L. Burnham, "Image analysis method for quantifying snow losses on PV systems," in *2020 47th IEEE Photovoltaic Specialists Conference (PVSC)*, IEEE, Jun. 2020, pp. 1510–1516. doi: 10.1109/PVSC45281.2020.9300373.

[109] R. E. Pawluk, Y. Chen, and Y. She, "Photovoltaic electricity generation loss due to snow – A literature review on influence factors, estimation, and mitigation," *Renew. Sustain. Energy Rev.*, vol. 107, pp. 171–182, Jun. 2019, doi: 10.1016/J.RSER.2018.12.031.

[110] T. Townsend and L. Powers, "Photovoltaics and snow: An update from two winters of measurements in the SIERRA," in *2011 37th IEEE Photovoltaic Specialists Conference*, IEEE, Jun. 2011, pp. 003231–003236. doi: 10.1109/PVSC.2011.6186627.

[111] B. Marion, R. Schaefer, H. Caine, and G. Sanchez, "Measured and modeled photovoltaic system energy losses from snow for Colorado and Wisconsin locations," *Sol. Energy*, vol. 97, pp. 112–121, Nov. 2013, doi: 10.1016/j.solener.2013.07.029.

[112] C. Baldus-Jeursen *et al.*, "Snow losses for photovoltaic systems: Validating the Marion and Townsend Models," *IEEE J. Photovoltaics*, pp. 1–11, 2023, doi: 10.1109/JPHOTOV.2023.3264644.

[113] M. B. Ogaard, I. Frimannslund, H. N. Riise, and J. Selj, "Snow loss modeling for roof mounted photovoltaic systems: Improving the Marion snow loss model," *IEEE J. Photovoltaics*, vol. 12, no. 4, pp. 1005–1013, Jul. 2022, doi: 10.1109/JPHOTOV.2022.3166909.

[114] M. van Noord, T. Landelius, and S. Andersson, "Snow-induced PV loss modeling using production-data inferred PV system models," *Energies*, vol. 14, no. 6, p. 1574, Mar. 2021, doi: 10.3390/en14061574.

[115] D. Gun, "Dynamic snow loss model and validation," in *2018 10th PV Performance Modeling Workshop*, 2018. [Online]. Available: https://pvpmc.sandia.gov/resources-and-events/events/2018-10th-pv-performance-modeling-workshop/

[116] R. W. Andrews, A. Pollard, and J. M. Pearce, "The effects of snowfall on solar photovoltaic performance," *Sol. Energy*, vol. 92, pp. 84–97, Jun. 2013, doi: 10.1016/j.solener.2013.02.014.

[117] E. C. Cooper, L. Burnham, and J. L. Braid, "Photovoltaic inverter-based quantification of snow conditions and power loss," *EPJ Photovoltaics*, vol. 15, p. 6, Feb. 2024, doi: 10.1051/epjpv/2024004.

[118] B. Rayegani, S. Barati, H. Goshtasb, S. Gachpaz, J. Ramezani, and H. Sarkheil, "Sand and dust storm sources identification: A remote sensing approach," *Ecol. Indic.*, vol. 112, no. October 2019, p. 106099, 2020, doi: 10.1016/j.ecolind.2020.106099.

[119] C. Opp, M. Groll, H. Abbasi, and M. A. Foroushani, "Causes and effects of sand and dust storms: What has past research taught us? A survey," *J. Risk Financ. Manag.*, vol. 14, no. 7, p. 326, 2021, doi: 10.3390/jrfm14070326.

[120] L. Micheli, F. Almonacid, J. G. Bessa, Á. Fernández-Solas, and E. F. Fernández, "The impact of extreme dust storms on the national photovoltaic energy supply," *Sustain. Energy Technol. Assessments*, vol. 62, p. 103607, Feb. 2024, doi: 10.1016/j.seta.2024.103607.

[121] R. Conceição *et al.*, "Saharan dust transport to Europe and its impact on photovoltaic performance: A case study of soiling in Portugal," *Sol. Energy*, vol. 160, no. September 2017, pp. 94–102, 2018, doi: 10.1016/j.solener.2017.11.059.

[122] S. J. Kramer, B. P. Kirtman, P. Zuidema, and F. Ngan, "Subseasonal variability of elevated dust concentrations over south Florida," *J. Geophys. Res. Atmos.*, vol. 125, no. 6, pp. 1–14, 2020, doi: 10.1029/2019JD031874.

[123] P. G. Kosmopoulos *et al.*, "Dust impact on surface solar irradiance assessed with model simulations, satellite observations and ground-based measurements," *Atmos. Meas. Tech.*, vol. 10, no. 7, pp. 2435–2453, Jul. 2017, doi: 10.5194/amt-10-2435-2017.

[124] M. J. Adinoyi and S. A. M. Said, "Effect of dust accumulation on the power outputs of solar photovoltaic modules," *Renew. Energy*, vol. 60, pp. 633–636, Dec. 2013, doi: 10.1016/j.renene.2013.06.014.

[125] W. Javed, B. Guo, B. Figgis, L. Martin Pomares, and B. Aïssa, "Multi-year field assessment of seasonal variability of photovoltaic soiling and environmental factors in a desert environment," *Sol. Energy*, vol. 211, pp. 1392–1402, Nov. 2020, doi: 10.1016/j.solener.2020.10.076.

[126] K. Papachristopoulou *et al.*, "15-year analysis of direct effects of total and dust aerosols in solar radiation/energy over the Mediterranean basin," *Remote Sens.*, vol. 14, no. 7, p. 1535, Mar. 2022, doi: 10.3390/rs14071535.

[127] Manajit Sengupta *et al.*, *Solar resource for high penetration and large scale applications: Fourth edition*. 2024. [Online]. Available: https://iea-pvps.org/research-tasks/solar-resource-for-high-penetration-and-large-scale-applications/#:$~$:text=The

[128] D. M. Giles *et al.*, "Advancements in the aerosol robotic network (AERONET) Version 3 database – Automated near-real-time quality control algorithm with improved cloud screening for Sun photometer aerosol optical depth (AOD) measurements," *Atmos. Meas. Tech.*, vol. 12, no. 1, pp. 169–209, Jan. 2019, doi: 10.5194/amt-12-169-2019.

[129] A. Gkikas *et al.*, "ModIs dust aerosol (MIDAS): A global fine-resolution dust optical depth data set," *Atmos. Meas. Tech.*, vol. 14, no. 1, pp. 309–334, 2021, doi: 10.5194/amt-14-309-2021.

[130] A. Inness *et al.*, "CAMS global reanalysis (EAC4)," Copernicus Atmosphere Monitoring Service (CAMS) Atmosphere Data Store (ADS). Accessed: Nov. 27, 2024. [Online]. Available: https://www.ecmwf.int/en/forecasts/dataset/cams-global-reanalysis

[131] A. Gkikas *et al.*, "The regime of intense desert dust episodes in the Mediterranean based on contemporary satellite observations and ground measurements," *Atmos. Chem. Phys.*, vol. 13, no. 23, pp. 12135–12154, 2013, doi: 10.5194/acp-13-12135-2013.

[132] Copernicus, "CAMS aerosol alerts." Accessed: May 15, 2024. [Online]. Available: https://aerosol-alerts.atmosphere.copernicus.eu/

[133] S. Bodenheimer, I. M. Lensky, and U. Dayan, "Characterization of Eastern Mediterranean dust storms by area of origin; North Africa vs. Arabian Peninsula," *Atmos. Environ.*, vol. 198, pp. 158–165, Feb. 2019, doi: 10.1016/j.atmosenv.2018.10.034.

[134] N. Middleton *et al.*, "A 10-year time-series analysis of respiratory and cardiovascular

morbidity in Nicosia, Cyprus: the effect of short-term changes in air pollution and dust storms," *Environ. Heal.*, vol. 7, no. 1, p. 39, Dec. 2008, doi: 10.1186/1476-069X-7-39.

[135] R. Givehchi, M. Arhami, and M. Tajrishy, "Contribution of the Middle Eastern dust source areas to PM10 levels in urban receptors: Case study of Tehran, Iran," *Atmos. Environ.*, vol. 75, pp. 287–295, Aug. 2013, doi: 10.1016/j.atmosenv.2013.04.039.

[136] L. Thalib and A. Al-Taiar, "Dust storms and the risk of asthma admissions to hospitals in Kuwait," *Sci. Total Environ.*, vol. 433, pp. 347–351, Sep. 2012, doi: 10.1016/j.scitotenv.2012.06.082.

[137] E. Ganor, A. Stupp, and P. Alpert, "A method to determine the effect of mineral dust aerosols on air quality," *Atmos. Environ.*, vol. 43, no. 34, pp. 5463–5468, Nov. 2009, doi: 10.1016/j.atmosenv.2009.07.028.

[138] A. Gkikas *et al.*, "Mediterranean intense desert dust outbreaks and their vertical structure based on remote sensing data," *Atmos. Chem. Phys.*, vol. 16, no. 13, pp. 8609–8642, Jul. 2016, doi: 10.5194/acp-16-8609-2016.

[139] C. Schill *et al.*, *Soiling losses – Impact on the performance of photovoltaic power plants report IEA-PVPS T13-21:2022*. 2022. [Online]. Available: https://iea-pvps.org/key-topics/soiling-losses-impact-on-the-performance-of-photovoltaic-power-plants/

[140] J. G. Bessa, L. Micheli, F. Almonacid, and E. F. Fernández, "Monitoring photovoltaic soiling: assessment, challenges, and perspectives of current and potential strategies," *iScience*, vol. 24, no. 3, p. 102165, Mar. 2021, doi: 10.1016/j.isci.2021.102165.

[141] M. Gostein, B. Littmann, J. R. Caron, and L. Dunn, "Comparing PV power plant soiling measurements extracted from PV module irradiance and power measurements," in *2013 IEEE 39th Photovoltaic Specialists Conference (PVSC)*, IEEE, Jun. 2013, pp. 3004–3009. doi: 10.1109/PVSC.2013.6745094.

[142] M. Z. Khan *et al.*, "Soiling mitigation potential of glass coatings and tracker routines in the desert climate of Saudi Arabia," *Prog. Photovoltaics Res. Appl.*, vol. 32, no. 1, pp. 45–55, Jan. 2024, doi: 10.1002/pip.3736.

[143] C. Sansom, P. King, A. Fernández-García, H. Almond, T. Kayani, and H. Boujjat, "The design of dust barriers to reduce collector mirror soiling in CSP plants," in *SolarPACES 2017: International Conference on Concentrating Solar Power and Chemical Energy Systems*, Santiago, Chile, 2018, p. 030017. doi: 10.1063/1.5067033.

[144] K. Ilse *et al.*, "Techno-economic assessment of soiling losses and mitigation strategies for solar power generation," *Joule*, vol. 3, no. 10, pp. 2303–2321, Oct. 2019, doi: 10.1016/j.joule.2019.08.019.

[145] A. Lemonsu, A. Beaulant, S. Somot, and V. Masson, "Evolution of heat wave occurrence over the Paris basin (France) in the 21st century," *Clim. Res.*, vol. 61, no. 1, pp. 75–91, Sep. 2014, doi: 10.3354/cr01235.

[146] G. A. Meehl and C. Tebaldi, "More intense, more frequent, and longer lasting heat waves in the 21st century," *Science*, vol. 305, no. 5686, pp. 994–997, 13 Aug. 2004, doi: 10.1126/science.1098704.

[147] Intergovernmental Panel on Climate Change (IPCC), "AR4 Climate change 2007: The physical science basis," Cambridge University Press, 2007. Accessed: Nov. 19, 2024. [Online]. Available: https://www.ipcc.ch/report/ar4/wg1/

[148] S. Jerez *et al.*, "The impact of climate change on photovoltaic power generation in Europe," *Nat. Commun.*, vol. 6, no. 1, p. 10014, Dec. 2015, doi: 10.1038/ncomms10014.

[149] S. Aivalioti, “Electricity sector adaptation to heat waves,” *Sabin Cent. Clim. Chang. Law, Columbia Law Sch. January 2015*, Jan. 2015, Accessed: May 20, 2024. [Online]. Available: https://scholarship.law.columbia.edu/sabin_climate_change/136

[150] K. Rüfer, “Considerations for solar projects during heat waves,” PV magazine International. Accessed: May 20, 2024. [Online]. Available: https://www.pv-magazine.com/2022/07/20/considerations-for-solar-projects-during-heat-waves/

[151] R. Regan, “Global heat wave puts solar panels to the test,” Solar Tribune. Accessed: May 20, 2024. [Online]. Available: https://solartribune.com/global-heat-wave-puts-solar-panels-to-the-test/

[152] K.-J. Ha *et al.*, “Dynamics and characteristics of dry and moist heatwaves over East Asia,” *npj Clim. Atmos. Sci.*, vol. 5, no. 1, p. 49, Jun. 2022, doi: 10.1038/s41612-022-00272-4.

[153] A. Porat, “Extreme heatwave 14 to 22 May 2020,” Israel Meteorological Service. Accessed: May 20, 2024. [Online]. Available: https://ims.gov.il/en/node/106

[154] I. Kaaya, M. Koehl, A. P. Mehilli, S. de Cardona Mariano, and K. A. Weiss, “Modeling outdoor service lifetime prediction of PV modules: Effects of combined climatic stressors on PV module power degradation,” *IEEE J. Photovoltaics*, vol. 9, no. 4, pp. 1105–1112, Jul. 2019, doi: 10.1109/JPHOTOV.2019.2916197.

[155] J. Ascencio-Vásquez, I. Kaaya, K. Brecl, K.-A. Weiss, and M. Topič, “Global climate data processing and mapping of degradation mechanisms and degradation rates of PV modules,” *Energies*, vol. 12, no. 24, p. 4749, Dec. 2019, doi: 10.3390/en12244749.

[156] M. Theristis, J. Stein, C. Deline, D. Jordan, C. Robinson, W. Sekulic, et al, Onymous early-life performance degradation analysis of recent photovoltaic module technologies, *Prog Photovolt Res Appl,* vol, 31, no. 2, pp. 149-160, April 2023, doi: 10.1002/pip.3615.

[157 G. Simpkins, “Extreme rain in India,” *Nat. Clim. Chang.*, vol. 7, no. 11, pp. 760–760, Nov. 2017, doi: 10.1038/nclimate3429.

[158] H. Upadhyaya, “Kerala floods: What to expect when none of the 61 dams have any emergency plan?,” DownToEarth. Accessed: Nov. 29, 2024. [Online]. Available: https://www.downtoearth.org.in/natural-disasters/kerala-floods-what-to-expect-when-none-of-the-61-dams-have-any-emergency-plan--61416

[159] “Floods, a deadly annual feature – How long before it sinks in,” DNA-India. Accessed: Nov. 29, 2024. [Online]. Available: https://www.dnaindia.com/india/report-floods-a-deadlyannual-feature-how-long-before-it-sinks-in-2654699

[160] N. Shiradkar, “Reliability and safety issues observed in flood affected PV power plants and strategies to mitigate the damage in future,” in *2019 IEEE 46th Photovoltaic Specialists Conference (PVSC)*, IEEE, Jun. 2019, pp. 3097–3102. doi: 10.1109/PVSC40753.2019.8981158.

[161] Intergovernmental Panel on Climate Change (IPCC), *Global warming of 1.5°C*. Cambridge University Press, 2018. doi: 10.1017/9781009157940.

[162] M. W. Jones *et al.*, “State of wildfires 2023–2024,” *Earth Syst. Sci. Data*, vol. 16, no. 8, pp. 3601–3685, Aug. 2024, doi: 10.5194/essd-16-3601-2024.

[163] United Nations Environment Programme, “Spreading like wildfire: The rising threat of extraordinary landscape fires,” 2022. Accessed: Nov. 19, 2024. [Online]. Available: https://www.unep.org/resources/report/spreading-wildfire-rising-threat-extraordinary-landscape-fires

[164] J. T. Abatzoglou, D. S. Battisti, A. P. Williams, W. D. Hansen, B. J. Harvey, and C. A. Kolden, “Projected increases in western US forest fire despite growing fuel constraints,” *Commun. Earth Environ.*, vol. 2, no. 1, p. 227, Nov. 2021, doi: 10.1038/s43247-021-00299-0.

[165] S. El Garroussi, F. Di Giuseppe, C. Barnard, and F. Wetterhall, “Europe faces up to tenfold increase in extreme fires in a warming climate,” *npj Clim. Atmos. Sci.*, vol. 7, no. 1, p. 30, Jan. 2024, doi: 10.1038/s41612-024-00575-8.

[166] L. Donaldson, D. M. Piper, and D. Jayaweera, “Temporal solar photovoltaic generation capacity reduction from wildfire smoke,” *IEEE Access*, vol. 9, pp. 79841–79852, 2021, doi: 10.1109/ACCESS.2021.3084528.

[167] S. D. Gilletly, N. D. Jackson, and A. Staid, “Quantifying wildfire-induced impacts to photovoltaic energy production in the western United States,” in *2021 IEEE 48th Photovoltaic Specialists Conference (PVSC)*, IEEE, Jun. 2021, pp. 1619–1625. doi: 10.1109/PVSC43889.2021.9518514.

[168] A. M. Nobre *et al.*, “On the impact of haze on the yield of photovoltaic systems in Singapore,” *Renew. Energy*, vol. 89, pp. 389–400, Apr. 2016, doi: 10.1016/J.RENENE.2015.11.079.D.

[169] E. Ford, I. M. Peters, and B. Hoex, “Quantifying the impact of wildfire smoke on solar photovoltaic generation in Australia,” *iScience*, vol. 27, no. 2, p. 108611, Feb. 2024, doi: 10.1016/j.isci.2023.108611.